

Toward Point-of-Care Drug Quality Assurance in Developing Countries: Comparison of Liquid Chromatography and Infrared Spectroscopy Quantitation of a Small-Scale Random Sample of Amoxicillin, Ciprofloxacin and Doxycycline.

Norah Alotaibi

Thesis submitted to the  
Faculty of Science  
University of Ottawa  
in partial fulfillment of the requirements for  
the degree of Master of Science in the  
Department of Chemistry and Biomolecular Sciences

December 2019

Candidate

Supervisor/Superviseur

Norah Alotaibi

Dr. Paul M. Mayer

## List of Publications

1. Alotaibi, Norah, Sean Overton, Sharon Curtis, Jason W. Nickerson, Amir Attaran, Sheldon Gilmer, and Paul M. Mayer. 2018. "Toward Point-of-Care Drug Quality Assurance in Developing Countries: Comparison of Liquid Chromatography and Infrared Spectroscopy Quantitation of a Small-Scale Random Sample of Amoxicillin." *American Journal of Tropical Medicine and Hygiene*.

List of authors and their roles on the project:

I ran all samples for amoxicillin, ciprofloxacin, and doxycycline on the FT-IR and quantified the results. I also performed the LC-UV analysis for doxycycline. I was involved in the data analysis for the three antibiotics, developing the discussion, and deriving the conclusion of the paper and the thesis.

Amir Attaran: Our collaborator in public health law

Jason Nickerson: Formerly of the Bruyere Research Institute, currently with Doctors Without Borders. He collected the non-African samples during his travels

Sean Overton: Sean collected samples in Ghana and Sierra Leone, taught me how to use the FTIR and LC-UV, ran all the LC-UV samples for amoxicillin and ciprofloxacin.

Sharon Curtis: JLH Facility Manager who ran the standard samples in the method validation.

Shelden Gilmer: The collaborator from World Hope Canada who escorted Sean Overton on his sampling trip to Ghana and Sierra Leone.

# Contents

List of Publications .....	ii
List of Figures .....	v
List of Tables .....	vi
List of Abbreviations .....	vii
Abstract .....	viii
Acknowledgements.....	ix
<b>1. Introduction .....</b>	<b>1</b>
<b>2. Experimental Techniques .....</b>	<b>6</b>
2.1 Infrared (IR) spectroscopy .....	6
2.2 Attenuated total reflectance (ATR) .....	9
2.3 IR spectroscopy of the target antibiotics .....	10
2.4 Calibration of FT-IR.....	13
2.5 High- and ultrahigh-performance liquid chromatography (HPLC-UV and UPLC-UV) .....	18
2.6 Calibration of LC-UV .....	22
<b>3. Amoxicillin trihydrate .....</b>	<b>23</b>
3.1 Structure .....	23
3.2 Chemical and physical properties .....	23
3.3 Materials and methods .....	24
3.3.1 Sampling.....	24
3.3.2 Sample preparation. ....	24
3.3.3 UPLC-UV protocol. ....	25
3.3.4 FT-IR protocol.....	26
3.4 Results and discussion .....	27
3.4.1 Total dose mass .....	27
3.4.2 UPLC-UV results .....	28
3.4.3 FT-IR results .....	29
3.4.4 UPLC vs FT-IR.....	30

<b>4. Ciprofloxacin Hydrochloride .....</b>	<b>31</b>
4.1 Structure .....	31
4.2 Chemical and physical properties .....	31
4.3 Materials and methods .....	32
4.3.1 Sampling.....	32
4.3.2 Sample preparation. ....	32
4.3.3 UPLC protocol. ....	33
4.3.4 FT-IR Protocol.....	34
4.4 Results and discussion .....	35
4.4.1 Total dose mass. ....	35
4.4.2 UPLC-UV results. ....	36
4.4.3 FT-IR results. ....	37
4.4.4 UPLC vs FT-IR.....	38
<b>5. Doxycycline hyclate .....</b>	<b>39</b>
5.1 Structure .....	39
5.2 Chemical and physical properties .....	39
5.3 Materials and methods .....	40
5.3.1 Sampling.....	40
5.3.2 Sample preparation. ....	40
5.3.3 UPLC protocol. ....	41
5.3.4 FT-IR protocol.....	42
5.4 Results and discussion .....	43
5.4.1 Total dose mass. ....	43
5.4.2 UPLC-UV results. ....	44
5.4.3 FT-IR results. ....	45
5.4.4 UPLC vs FT-IR.....	46
<b>6. Conclusions .....</b>	<b>48</b>
<b>Bibliography.....</b>	<b>50</b>

**Appendix**

- A1. Raw results for amoxicillin
- A2. Raw results for ciprofloxacin
- A3. Raw results for doxycycline

## List of Figures

Figure 2.1: The components of a simple dispersive infrared spectrometer, based on ref. 19. <sup>19</sup> ...	7
Figure 2.2: The components of FT-IR, based on ref. 19. <sup>19</sup> .....	8
Figure 2.3: How ATR works, based on ref. 23. <sup>23</sup> .....	10
Figure 2.4: The experimental IR vs. the theoretical IR spectra (B3-LYP/6-31+G(d) level of theory) for amoxicillin ciprofloxacin, and doxycycline. ....	11
Figure 2.5: IR spectra of a) amoxicillin, b) ciprofloxacin, and c) doxycycline and the calibration mixtures with a calibration curve taken at a single wavelength to demonstrate linearity for amoxicillin. ....	17
Figure 2.6: An example of a spectrum obtained by LC-UV for ciprofloxacin. ....	19
Figure 2.7: The calibration curve for ciprofloxacin with the regression equation and R2 value" error bars are smaller than the symbol size". ....	22
Figure 3.1: The structure of amoxicillin. <sup>28</sup> .....	23
Figure 3.2: Mass results by countries. ....	27
Figure 3.3: The LC-UV results for amoxicillin by countries. ....	28
Figure 3.4: The FT-IR results for amoxicillin by countries. ....	29
Figure 3.5: %API of amoxicillin by LC-UV vs. FT-IR. ....	30
Figure 4.1: The structure of ciprofloxacin. <sup>32</sup> .....	31
Figure 4.2: The mass results for ciprofloxacin by countries. ....	35
Figure 4.3: The LC-UV results for ciprofloxacin by countries. ....	36
Figure 4.4: The FT-IR results for ciprofloxacin by countries. ....	37
Figure 4.5: %API of ciprofloxacin by LC-UV vs. FT-IR. ....	38
Figure 5.1: The structure of doxycycline. <sup>34</sup> .....	39
Figure 5.2: The mass results for doxycycline by countries. ....	43
Figure 5.3: The LC-UV results for doxycycline by countries. ....	44
Figure 5.4: The FT-IR results for doxycycline by countries. ....	45
Figure 5.5: %API of doxycycline by LC-UV vs. FT-IR .....	46

## List of Tables

Table 1: The infrared regions and their wavelength and wavenumber range. <sup>22</sup> .....	6
Table 2: Selected vibrational frequencies of the functional groups in the IR spectrum of amoxicillin.....	12
Table 3: Selected vibrational frequencies of the functional groups in the IR spectrum of ciprofloxacin. ....	12
Table 4: Selected vibrational frequencies of the functional groups in the IR spectrum of doxycycline. ....	13

## List of Abbreviations

API: Active Pharmaceutical Ingredient

ATR: Attenuated Total Reflectance

DRC: Democratic Republic of Congo

FT-IR: Fourier Transform Infrared

HPLC: High-Performance Liquid Chromatography

PLS: Partial Least Squares

PNG: Papua New Guinea

UPLC: Ultra High-Performance Liquid Chromatography

USP: United States Pharmacopoeia

UV: Ultraviolet, used to represent ultraviolet-visible spectroscopy detection of the UPLC

VWD: Variable Wavelength Detector

WHO: The World Health Organization

## Abstract

Substandard antibiotics are thought to be a major threat to public health in developing countries and a cause of antimicrobial resistance. However, assessing quality outside of a laboratory setting, using simple equipment, is challenging. The aim of this study was to validate the use of a portable Fourier transform infrared (FT-IR) spectrometer for the identification of substandard antibiotics. Results are presented for amoxicillin, ciprofloxacin, and doxycycline packages from Haiti, Ghana, Sierra Leone, Democratic Republic of Congo, India, Papua New Guinea, and Ethiopia collected over the course of 6 months in 2017, including two field trips with the FT-IR to Ghana and Sierra Leone. Canadian samples were used as a control. Regarding drug quality, of 290, 280, and 42 individual capsules and tablets of amoxicillin, ciprofloxacin, and doxycycline analyzed, 13, 14, and 27 respectively were found to be substandard with total active pharmaceutical ingredients (API) lying outside the acceptable range of 90–110%. The FT-IR reliably identified the outliers of amoxicillin and ciprofloxacin and was found to yield results in good agreement with the established pharmacopeia liquid chromatography protocol. Results for doxycycline were less promising, but LC-UV analysis was also found to be problematic. We conclude that the portable FT-IR may be suitable to intercept substandard antibiotics in developing countries where more sophisticated techniques are not readily available.

## Acknowledgements

All praise the Almighty Allah for giving me the strength and ability to complete this journey.

I would like to express my very profound gratitude to my parents and siblings for their endless support, unconditional love, and prayers to complete this journey. Most of all, my appreciation goes to my husband and lovely daughter for providing me with unfailing support and continuous encouragement throughout my years of study and through the process of researching and writing this thesis. This accomplishment would not have been possible without them.

There are no words that can express how thankful I am to my supervisor, Prof. Paul Mayer, for allowing me to be in his research group and for guidance and continuous support. I would also like to express my thanks to Sean Overton for his assistance in the project and helping in numerical analysis. I also wish to thank Dr. Sharon Curtis for valuable assistance in the research. Special thanks to Dr. Brandi West for her help, assistance, and the great time we spent in the office.

My sincere thanks are also extended to the Ministry of Education in Saudi Arabia represented by the Saudi Arabian Cultural Bureau in Canada for financial support.

Finally, my grateful thanks go to my friends Shaimaa Almalki and Nouf Almohammadi, for helping, supporting, being a good listener, and all the great time I have spent with them in Ottawa.

# Chapter 1

## Introduction

Note. Taken largely from the paper discussed in the list of publications

In recent years, evidence has emerged that the problem of substandard medicines is large and growing.<sup>1</sup> These medicines, which may contain the wrong amount or type of ingredients, can cause drug resistance, injury, and death—sometimes hundreds of patients at a time. Little is known about the true dimensions of this issue and which patients or medicines it targets, although work by the World Health Organization (WHO) and INTERPOL roughly estimates that it affects between 1% and 30% of drugs.<sup>2</sup> Loopholes in law and regulation let wrongdoers trade bad-quality drugs, with little risk of punishment. INTERPOL notes that police reports of medicine crime are up 10-fold since 2000, sometimes causing hundreds of deaths.<sup>3</sup> Serious as that is, the WHO laments that current data on medicine quality “are often of poor quality and are not ... systematized.”<sup>2</sup> Pezzola and Sweet, in a study developing indicators for pharmaceutical regulation in developing countries, have noted resistance to the implementation of quality standards.<sup>4</sup> Even neighboring countries can have wildly different levels of regulation.<sup>4</sup> Jason W., Nickerson et al. have corroborated these concerns in small-scale exploratory studies that clearly illustrate the grave risks of treatment failure, drug resistance, and death. For example, they linked a specific vial of substandard antibiotic ceftriaxone in a Ugandan hospital to a young boy’s death in that hospital.<sup>5</sup> In addition, Nickerson, Jason W. et al. recently published on the identification of substandard propofol in Zambia, which was identified because of concerns of drug quality following several adverse events on administration, ranging from bronchospasm to hypotension

and cardiac arrest.<sup>6</sup> The literature contains little data on medicine testing in most disease areas (e.g., almost no published studies of noncommunicable-disease drugs), which in turn means there is not an evidence base that politicians find compelling enough to strengthen the laws and law enforcement needed to effectively criminalize and punish those who traffic substandard medicines. Nayyar and coworkers<sup>7,8</sup> published reviews in 2012 and 2015, highlighting the significance of falsified pharmaceuticals worldwide and the detection strategies that have been used. In addition to the high-performance liquid chromatography (HPLC) pharmacopeia standard methods, colorimetric and thin-layer chromatographies are two of the more common testing methods, less expensive, rapid, field-adapted and require no trained personnel. However, there are some drawbacks to each of them. Colorimetric techniques need sample pre-treatment. If the medicines do not have particular chemical groups that easily react with specific reagents to yield colored products, they can be transformed by acid or base treatment to more reactive compounds. Also, the specificity of the test is pH-dependent. Finally, colorimetry does not provide information on the chemical composition of counterfeit medicines. The thin-layer chromatography provides a semiquantitative measurement.

Fatal consequences and promoting the emergence of drug resistance are results of substandard or intentionally adulterated medicinal products in low-income countries.<sup>1</sup> For example, poor-quality antimalarial medicines contribute to emerging antibiotic resistance and treatment failure. Because when the antibiotic concentration is lower than what is needed, it will not kill all the bacteria. Instead, substandard medicine use promotes the development of antibiotic-resistant bacteria. Thus, poor-medicine effectively selecting bacteria that is resistant to the antibiotic and allowing them to survive to grow and continue to multiply, causing more

harm. Then over time, the bacteria will show resistance to that drug.<sup>9</sup> This not only endangers patient safety but consequently risks the loss of patients' trust in the health care system. In many low-income countries, drugs with little or no active ingredient, including first-line therapies for the treatment of tuberculosis, malaria and human immunodeficiency viruses, have been found.<sup>10</sup> In 21 countries of sub-Saharan Africa, 21 studies reporting chemical analyses and assessments of the packaging of antimalarial drugs showed that 796 (35%) of 2297 failed chemical analysis, 28 (36%) of 77 failed packaging analysis, and 79 (20%) of 389 were classified as falsified.<sup>7</sup> A study from the major cities of six African countries highlighted similar quality concerns, finding that 35% of all samples tested were outside acceptable quality ranges.<sup>11</sup> In 2008, a total of 1080 samples of oral antimalarial tablets purchased from retail outlets across 21 districts in mainland Tanzania to determine the amount of the active ingredient and dissolution profile by following the published United States Pharmacopoeia (USP) monogram for the particular tablet being tested. Overall 38 out of 1080 or 12.2% of the samples did not comply within the tolerance limits of the dissolution and quantification analysis.<sup>12</sup>

A limitation of most studies in the literature is that they are carried out after a patient or patients have been harmed by substandard dosing (as was performed in our previous work). This is a consequence of gold standard quantitative analysis being laboratory-based, and it points to a need for more portable, cost-effective, and user-friendly methods if this type of analysis is to be performed in a preventative manner.<sup>13</sup> Portable near-infrared (IR) and Raman spectroscopy devices have been deployed with mixed success, with quantitation of the active pharmaceutical ingredient (API) being most challenging.<sup>13-18</sup> This means that portable Raman and NIR instruments work in different fields; however, there are some limitations in each study. For

example, a study reviewed the recent analytical methods employed to control the quality of drug formulations, using artemisinin derivatives as an example, mentioned that portable Raman and NIR instruments for the in-field chemical identification of counterfeit drugs have now become available. Still, the practical advantage of the Raman technique is limited by the poor efficiency of the Raman scattering and strong fluorescent interferences. A significant drawback for the implementation of portable NIR spectrometers in resource-poor settings (but not in developed countries) is the need to process the spectral data by chemometric techniques to differentiate between original and fake formulations.<sup>13</sup> IR spectroscopy has been used to probe paracetamol tablets, over the fingerprint region 1,100–2,400  $\text{cm}^{-1}$ .<sup>19</sup> The authors determined that once a database of drugs had been developed, it was possible to demonstrate the reliability of a sample quickly and efficiently.

We have chosen to use Fourier-transform IR (FT-IR) spectroscopy over an extended wavelength range to better capture the IR spectrum and identify changes to excipient composition, thus hopefully limiting false negatives and positives. To this end, we partnered with Agilent Technologies, Inc. to develop one of their portable FT-IR spectrometers (Agilent 4500) for the identification of substandard antibiotics. In my thesis, we focus on the results obtained with the FT-IR and standard laboratory testing for amoxicillin capsules, ciprofloxacin tablets, and doxycycline collected over the course of 6 months from Haiti, Ghana, Sierra Leone, Papua New Guinea, the Democratic Republic of Congo (DRC), India, Ethiopia, and Indonesia. The pharmacopeia standard HPLC method was also used to serve as a validation for the FT-IR results, especially because the IR spectra are sensitive to excipients found in the capsules and tablets. There are two main motivations to choose amoxicillin, ciprofloxacin, and doxycycline. First, they

are the primary antibiotics used in most countries. Second, they represent the biggest families of antibiotics (penicillin, quinolones and tetracyclines, respectively). We concentrated on developing countries because pharmaceutical regulation is weaker there and pharmaceutical factories are more likely to have quality-control problems. The work for amoxicillin presented here has been already published in the paper mentioned above in the list of publications.

## Chapter 2

### Experimental Techniques

#### 2.1 Infrared (IR) spectroscopy<sup>20-22</sup>

Infrared (IR) spectroscopy studies the interaction between infrared radiation and matter. IR radiation is a part of the electromagnetic spectrum that has a longer wavelength than visible light. A longer wavelength means light carries less energy. IR spectroscopy can be subdivided, depending on the wavelength, into near, mid and far infrared (see Table 1), although mid-infrared is usually meant when the term IR spectroscopy is used.

Table 1: The infrared regions and their wavelength and wavenumber range.<sup>22</sup>

Regions	Wavelength range (nm)	Wavenumber range (cm <sup>-1</sup> )
Near-IR	780–2500 nm	13,500–4000
Mid-IR	2500–25,000	4000–400
Far-IR	25,000–1,000,000	400–10

IR light interacts with matter by being absorbed by specific vibrational modes. There are different kinds of molecular vibration including symmetric stretching, anti-symmetric stretching and deformation vibrations. Other vibrations are rocking, wagging and twisting vibrations.

For measuring the IR spectrum:

- 1- IR radiation is generated by a light source and directed at the sample.
- 2- While some light is reflected, the sample absorbs specific amounts of the light.

3- The remaining light is transmitted and collected by a detector to produce an electronic signal.

Turning the electronic signal to a spectrum depends on how the IR spectrometer set up. The dispersive IR spectrometer generates infrared radiation from a hot wire and splits it into two parallel beams by way of mirrors (Figure 2.1). One of the parallel beams passes through the sample, and the other beam is used as a reference. Then each beam is alternately dispersed by a diffraction grating, which transmits a selected wavelength to the detector. The difference between the sample and reference signals constitutes the recorded intensity at that wavelength. Rotating the diffraction grating passes differing wavelengths to the detector until the entire difference spectrum is acquired. Figure 2.1 schematically illustrates the components of a simple dispersive IR spectrometer. However, Fourier-transform infrared spectrometers offer significant advantages. They have improved signal to noise ratio, and they are a faster acquisition of IR spectra.

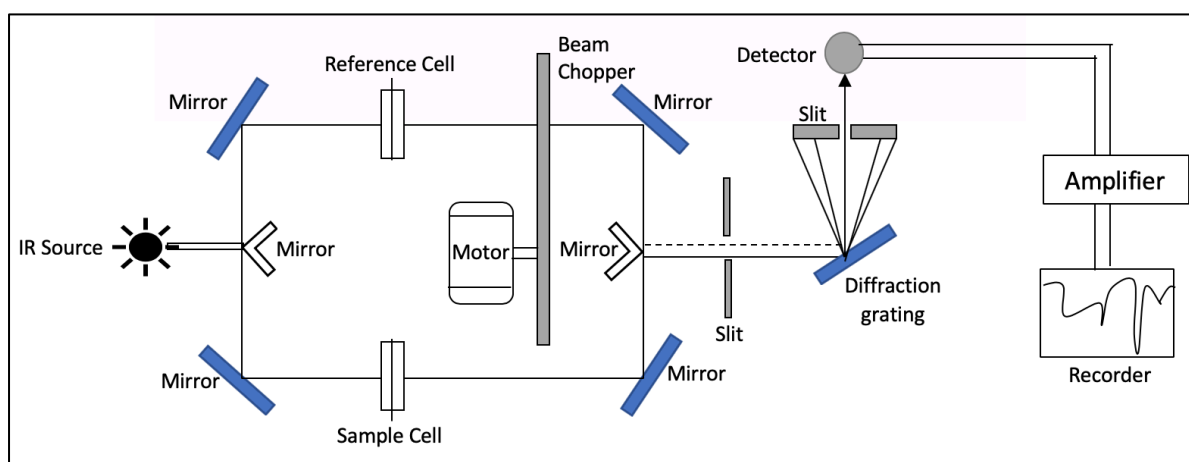


Figure 2.1: The components of a simple dispersive infrared spectrometer, based on ref. 19.<sup>19</sup>

The FT-IR spectrometer differs from a dispersive IR spectrometer. A schematic diagram of an FT-IR spectrometer is shown in Figure 2.2. The center of an FT-IR spectrometer is the Michelson interferometer. During the measurement, the IR beam enters the interferometer and is directed at the beam-splitter. The beam is then split and directed at a fixed and a moving mirror. The light travels back to the beam-splitter where it recombines causing interference and finally directed at the sample material. That way all the spectral information of all wavelengths is acquired simultaneously saving a lot of time. At the end, the detector produces a signal of light intensity versus mirror position.

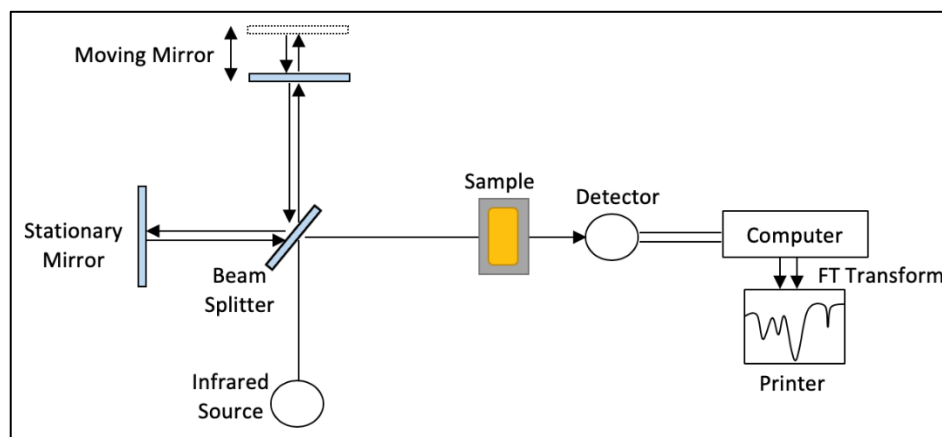


Figure 2.2: The components of FT-IR, based on ref. 19.<sup>19</sup>

To get a sample's IR spectrum, environmental influences are first recorded (the "blank"). The raw signal, called an interferogram, is then mathematically Fourier-transformed into a classical IR plot of light intensity versus wavenumbers. The sample spectrum is then recorded. Combining both spectra by subtraction results in the classic view of the FT-IR transmission spectrum.

An FT-IR spectrum is like a chemical fingerprint. This enables chemical identification of a variety of samples and is frequently used to characterize material properties and identify and verify known and unknown samples. It is utilized by many chemical and manufacturing industries but especially useful whenever chemical information needs to be obtained in a straightforward and short amount of time. FT-IR is extremely versatile, depending on the spectrometer setup and measuring technique used.

## **2.2 Attenuated total reflectance (ATR)**

The most commonly used FT-IR sampling instrument today employs attenuated total reflectance (ATR). ATR usually enables qualitative or quantitative sample analysis with little or no sample preparing that significantly accelerates sample analysis. The primary advantage of ATR sampling is the thin sampling path length of the IR beam. This is contrary to traditional transmission FT-IR sampling where the sample must be diluted with an IR transparent salt or solvent, pressed into a pellet or pushed into a thin film before analyzing to avoid fully absorbing bands in the infrared spectrum.<sup>23</sup>

### **2.2.1 How ATR works**

With the ATR accessory, the sample is placed on a diamond of high refractive index. The IR beam is directed into the diamond. The IR beam reflects from the internal surface of the crystal and creates an evanescent wave. The sample absorbs some of the energy of the reflected beam, and the rest of the reflected radiation returns to the detector, thereby “attenuating” the beam. Figure 2.4 demonstrates how the ATR accessory operates.

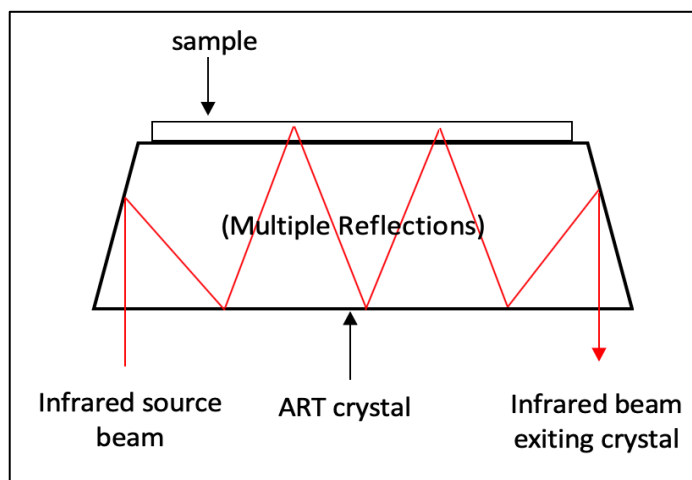


Figure 2.3: How ATR works, based on ref. 23.<sup>23</sup>

A nearly identical spectrum is acquired from both ATR-FT-IR and FT-IR working in the transmission mode. Also, the peak position in wavenumbers is the same in both methods. However, some variations in the comparative intensities of the peaks may be observed.

### 2.3 IR spectroscopy of the target antibiotics

The IR spectrum of a compound is a plot of absorption intensity versus wavenumber (or sometimes wavelength). In the spectrum, the shape and fine structure of a peak often give clues to its identity. For instance, C=O and C=C bonds absorb in the same region of the infrared spectrum. To distinguish between them the C=O bond is a strong absorber while the C=C bond is weak absorber. Consequently, the peak characteristics in the IR spectrum is as important as the frequency. The fingerprint region is important because each different compound produces its own unique pattern of peaks in this region. Once we identify an unknown compound, we compare its IR spectrum with that of a known sample of the compound. If all peaks in the fingerprint region match, we have identified our compound. Figure 2.4 displays the comparison

between the experimental and theoretical IR spectra for amoxicillin, ciprofloxacin, and doxycycline respectively.

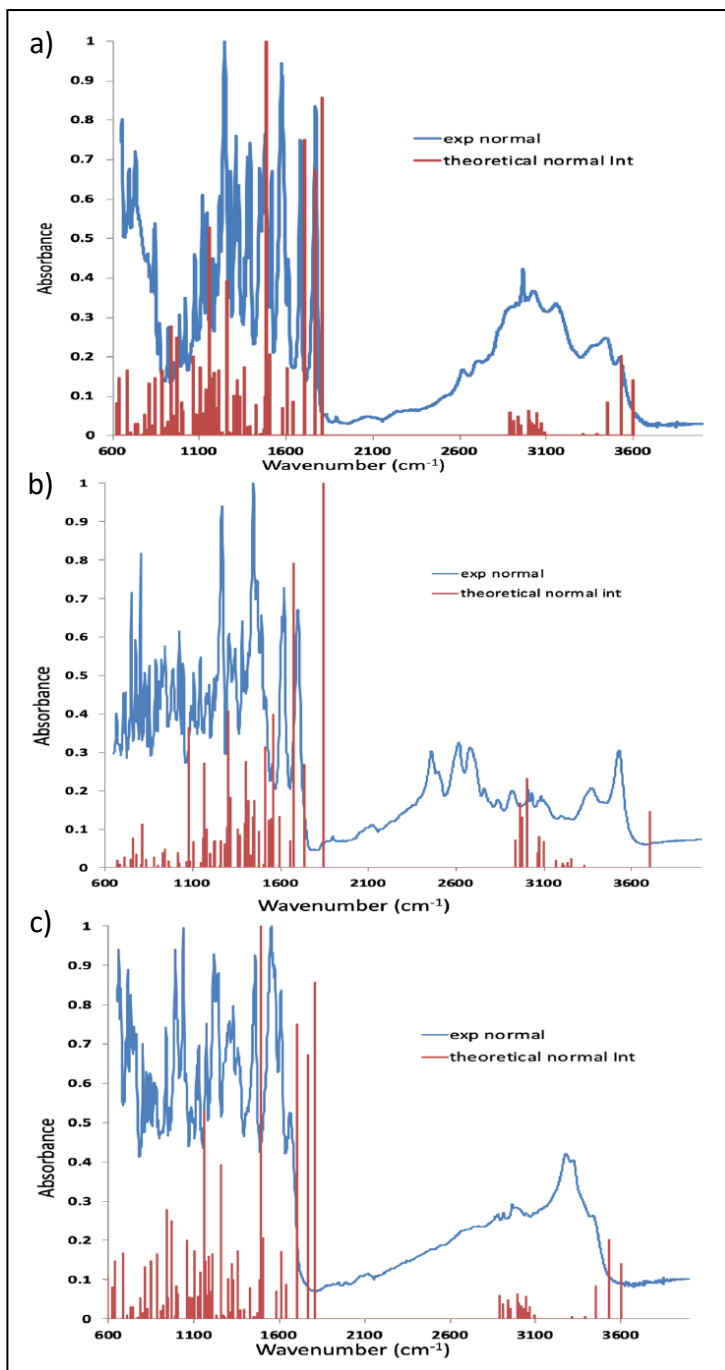


Figure 2.4: The experimental IR vs. the theoretical IR spectra (B3-LYP/6-31+G(d) level of theory) for a) amoxicillin, b) ciprofloxacin, and c) doxycycline.

Therefore, due to the functional group vibrations that appear in the IR spectra (Figure 2.5), we selected the fingerprint region of amoxicillin, ciprofloxacin, and doxycycline for quantitation. The tables below classify the chemical vibration of the functional groups in the IR spectrums for amoxicillin, ciprofloxacin, and doxycycline, respectively.

Table 2: Selected vibrational frequencies of the functional groups in the IR spectrum of amoxicillin.

<b>Bond</b>	<b>Start wavenumber (cm<sup>-1</sup>)</b>	<b>End wavenumber (cm<sup>-1</sup>)</b>
C-H in- plane def	1300	1200
C=C and S=N Stretch	1450	1410
C=C and C=N Stretch	1520	1470
C=C and C=N Stretch	1615	1570
C-H Stretch	3100	3010

Table 3: Selected vibrational frequencies of the functional groups in the IR spectrum of ciprofloxacin.

<b>Bond</b>	<b>Start wavenumber (cm<sup>-1</sup>)</b>	<b>End wavenumber (cm<sup>-1</sup>)</b>
COC symmetric stretch	1190	1130
COC antisymmetric stretch	1315	1260
C-H Bend, CH <sub>2</sub> /CH <sub>3</sub>	1480	1410
C=C Stretch	1645	1580
C=O Stretch	1740	1700
C-H Stretch, Alkyl	3000	2890
C-H Stretch, olefinic	3040	3010

Table 4: Selected vibrational frequencies of the functional groups in the IR spectrum of doxycycline.

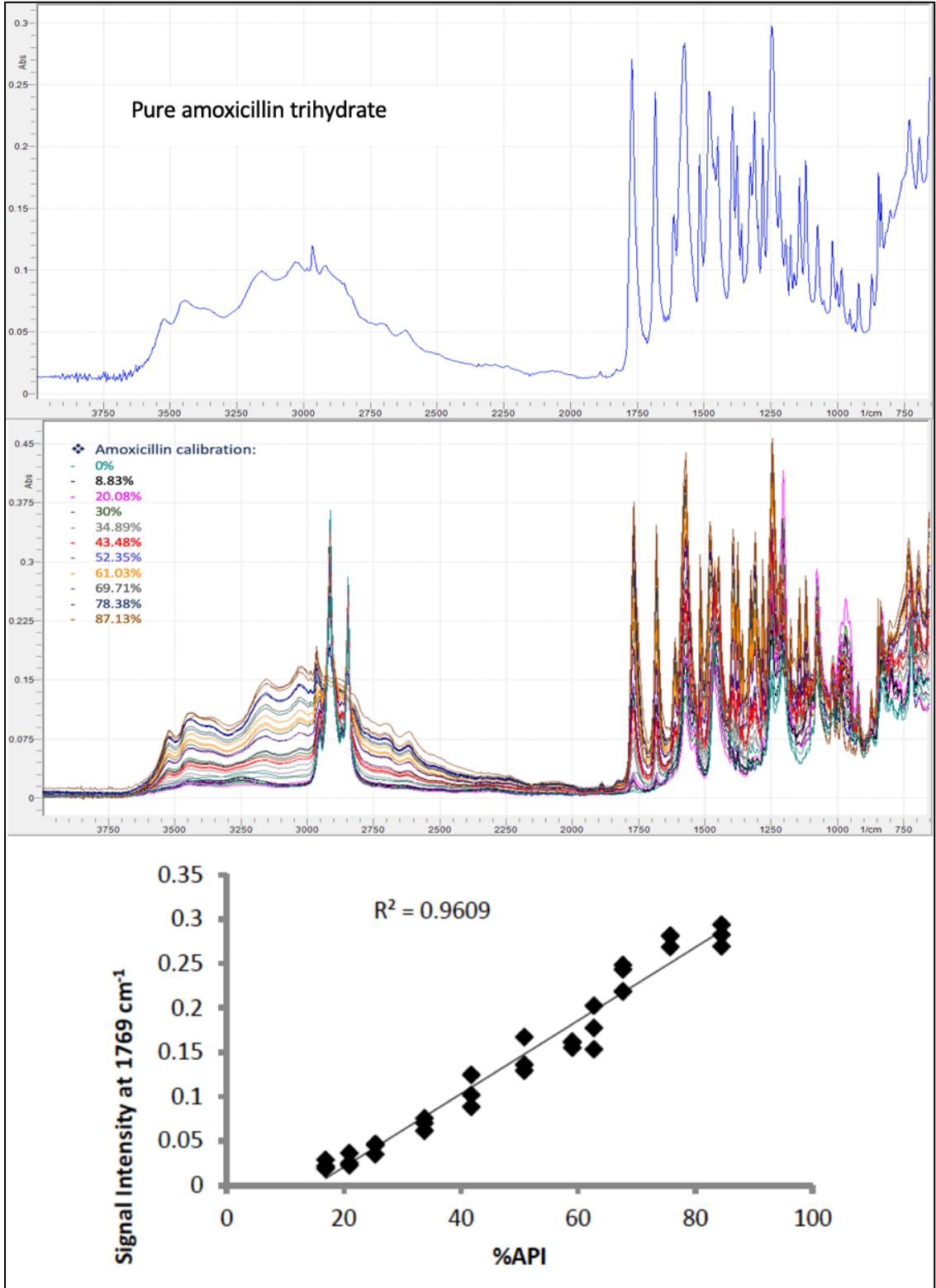
<b>Bond</b>	<b>Start wavenumber (cm<sup>-1</sup>)</b>	<b>End wavenumber (cm<sup>-1</sup>)</b>
C-C/C-S Stretch, Ring	1445	1395
C-C/C-S Stretch, Ring	1565	1515
C-H Stretch, Aryl	3115	3050

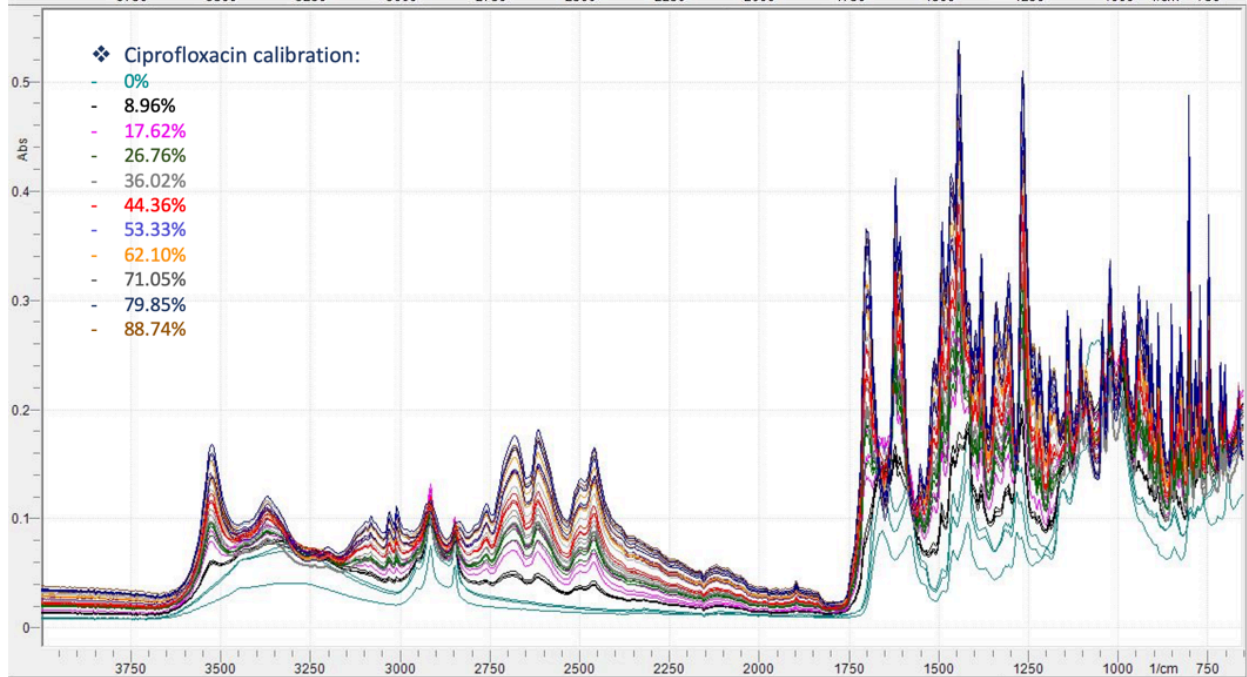
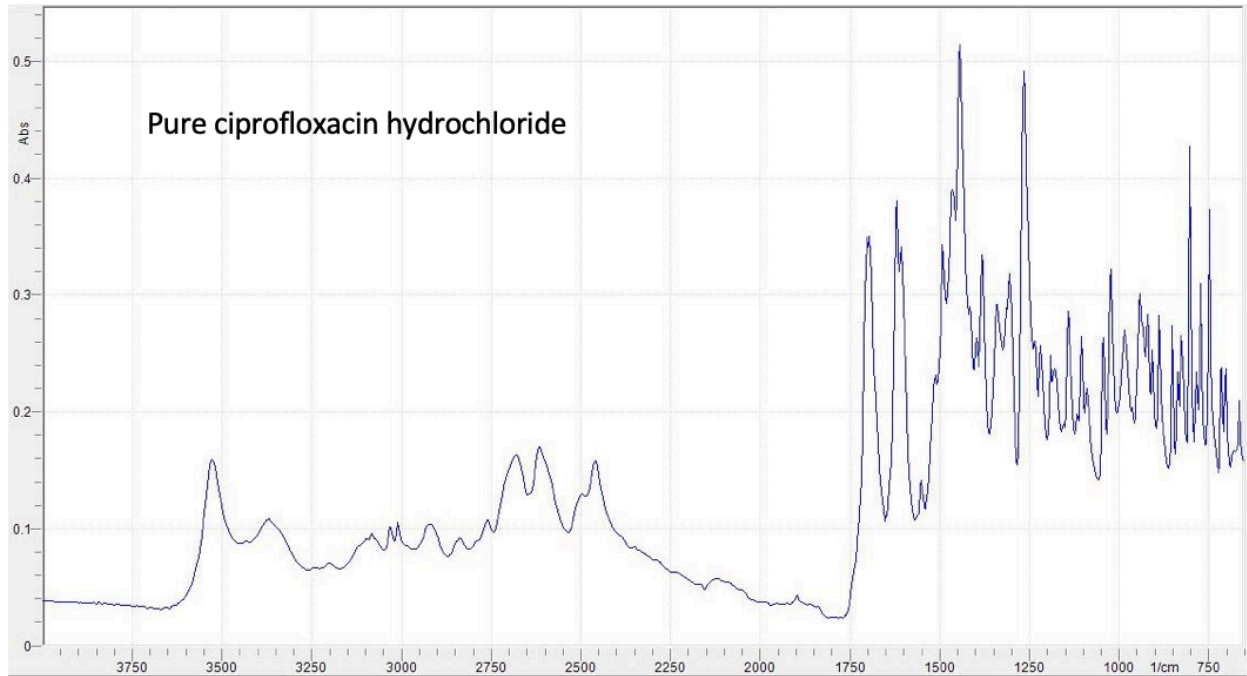
## 2.4 Calibration of FT-IR

Calibration curves of %w/w for the FT-IR samples were made from 12 or 11 points of different weights of standard drug and the excipients matrix (for more detail on how the excipient matrices are prepared, see the FT-IR protocol for each antibiotic. The standards are run in triplicate in the FT-IR and a partial least squares multiple linear regression calibration model was made using Agilent's MicroLab Expert. The fingerprint regions from the IR spectra are selected and used for calibration. Partial Least Squares (PLS) is an analytical tool to make predictions based on measurements comprising multiple (potentially hundreds) of responses that are highly co-linear. Developed in the 1960's by Herman Wold for economics, it has been applied to process monitoring involving hundreds of controllable variables with multiple outcomes. In spectroscopy, PLS is used to take each measured frequency in a spectrum of an analyte mixture and compare it to the calibration set of known relationship between the analyte and the "impurities". In the present case, the impurities are the excipients. PLS factors are calculated as a linear combination of spectral peak amplitudes. Thus, the process is distinct from

selecting one, or even ten, key wavelengths for quantitation. PLS literally uses every measured frequency of the selected spectral range.<sup>24</sup>

Examples of the IR spectra of pure amoxicillin, ciprofloxacin and doxycycline and the calibration mixtures for each antibiotic are found in Figure 2.5, together with a calibration curve taken at a single wavelength to demonstrate linearity for amoxicillin.





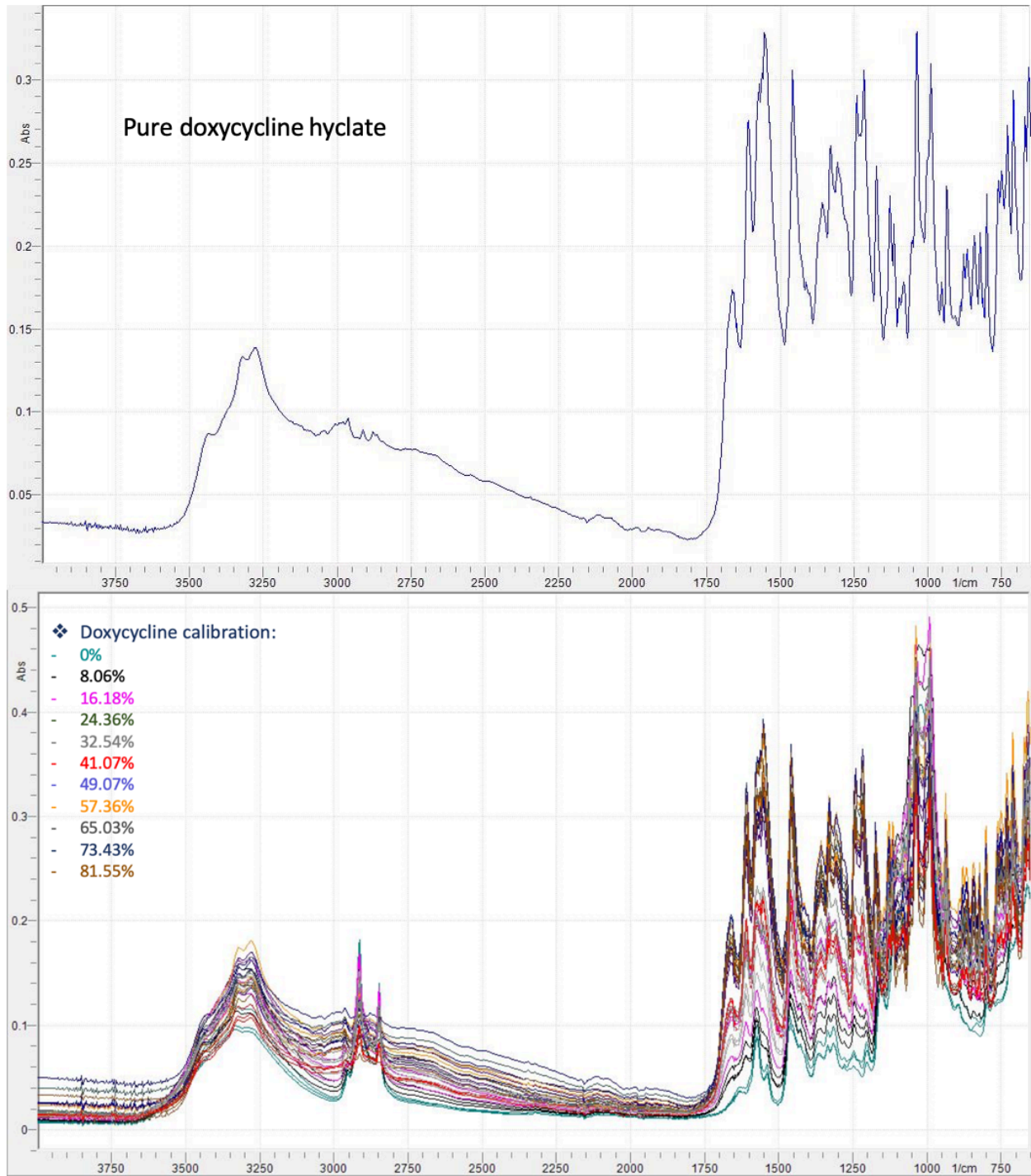


Figure 2.5: IR spectra of amoxicillin, ciprofloxacin, and doxycycline and the calibration mixtures with a calibration curve taken at a single wavelength to demonstrate linearity for amoxicillin.

Characteristic regions on the spectrum for each antibiotic (the fingerprints) were identified where there was little or no absorbance from excipient materials. In our IR spectra for the three antibiotics, we noticed that the excipients dominated the region 2700-3000  $\text{cm}^{-1}$ .

## **2.5 High- and ultrahigh-performance liquid chromatography (HPLC-UV and UPLC-UV)<sup>25</sup>**

### **2.5.1 How Liquid Chromatography (LC) Works<sup>26,27</sup>**

The sample mixture to be separated and analyzed is introduced into the flow path of the mobile phase and passes to a cartridge or column packed with a stationary phase. When the mobile phase moves through the column, the sample band separates into individual analyte bands. The time between injection and detection of an analyte is its retention time. The retention time of the samples will vary depending on the interaction between the stationary phase, the molecules being analyzed, and the solvent or solvents used. Analytes having the least amount of interaction with the stationary phase leave the column more rapidly. An example of a spectrum obtained by LC-UV for ciprofloxacin is shown in Figure 2.6.

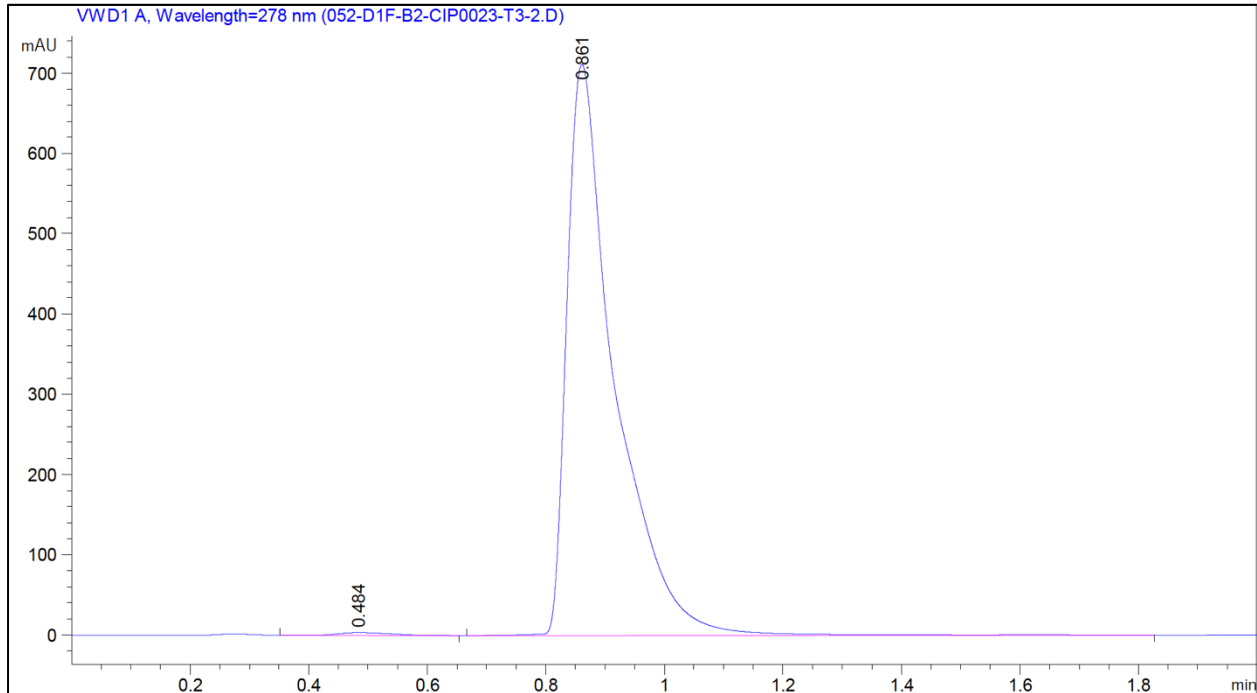


Figure 2.6: An example of a spectrum obtained by LC-UV for ciprofloxacin.

The Van Deemter equation that governs chromatographic performance:

$$HETP = A + \frac{B}{u} + C_s u + C_m u$$

Where:

- HETP = Height equivalent theoretical plate (plate height)
- A = Eddy-diffusion term
- B = longitudinal diffusion term
- C = Resistance to mass transfer term
- u = Linear velocity of the mobile phase

**Height equivalent theoretical plate:** is a result of normalizing the efficiency of a chromatography column with the length of the column. Plate height is the distance between successive partitions by the analyte with the stationary phase.

**Eddy diffusion:** describes the peak broadening due to the presence of stationary phase particles in the column. Eddy diffusion occurs as a result of multiple flow paths through a packed column bed.

**Longitudinal diffusion:** refers to the diffusion of individual analyte molecules in the mobile phase along the longitudinal direction of a column. Longitudinal diffusion contributes to peak broadening only at very low flow rates below the minimum plate height.

**The C-term:** relates to the mass transfer of sample components between the stationary phase and the mobile phase during separation. There are two separate mass transfer terms:

**C<sub>m</sub>-term:** describing the contributions to peak broadening in the mobile phase.

**C<sub>s</sub>-term:** describing the contributions to peak broadening in the stationary phase.

Resistance to mass transfer is dependent on the speed with which the partition equilibrium between mobile and stationary phases is obtained.

We can see that column performance is proportional to particle size, as shown by the components of the Van Deemter equations:

$$A = \lambda d_p \quad \text{and} \quad C_M \propto d_p^2 / D_M$$

Where:

$\lambda$ : is particle shape

$d_p$ : Particle size or particle diameter; the larger the particles, the stronger the dispersion effect.

$D_M$ : Diffusion coefficient of analyte in the mobile phase

Therefore, if the size of the particles decreases, the magnitude of the Eddy diffusion term and the mass transform into the mobile phase term can be dropped, and the plate height decreases. So, columns with small particles (less than 2 $\mu\text{m}$ ) provide higher resolution and better efficiency than the conventional ones. Also, they require high pressure to deliver the mobile phase. Thus, there has been a move away from high-performance liquid chromatography (HPLC) toward ultra-high-performance liquid chromatography (UPLC). The particle size used in HPLC is generally ranged between 3 and 50  $\mu\text{m}$  with 5  $\mu\text{m}$  particles being the most popular, while the particle size used in UPLC is sub-3  $\mu\text{m}$ . The pump designed to deliver the mobile phase in the 2 to 400 bar pressure range in HPLC, while in UPLC designed to deliver the mobile phase at 15,000 psi (1000 bar). Also, the peak resolution in UPLC higher than in HPLC because the column dimension of UPLC is smaller than in HPLC. In addition, UPLC delivers separations in 3 to 10 minutes, as compared to 15 to 20-minute separations in traditional HPLC. Consequently, UPLC technology facilitates improvements of resolution, sensitivity and speed to be achieved, without compromise. HPLC and UPLC are suitable for a wide variety of applications, including pharmaceuticals and food processing. It is particularly useful for organic compounds that are low or non-volatile and cannot be treated with gas chromatography.

## 2.6 Calibration of LC-UV

For the calibration curve, standard solutions of each antibiotic were injected into the UPLC system with different concentration and run five times (e.g. 0.272, 0.510, and 0.830 mg/ml for ciprofloxacin). Then the calibration graph was obtained by plotting peak area versus concentration. The linear regression for ciprofloxacin is presented in Figure 2.7.

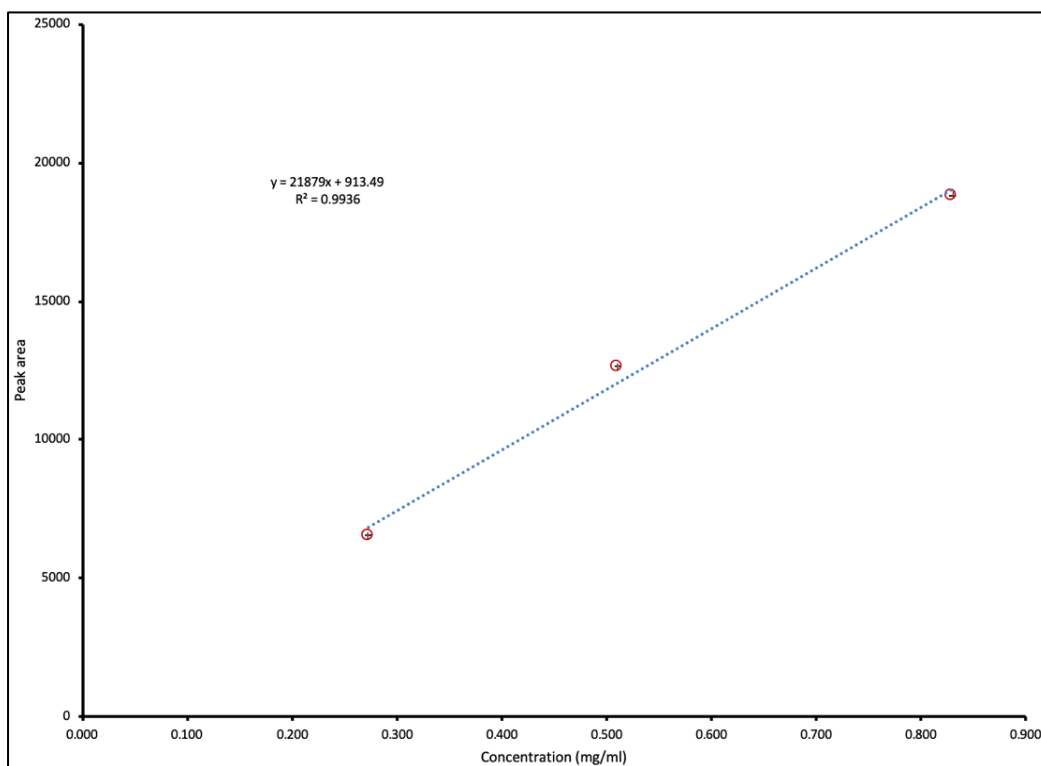


Figure 2.7: The calibration curve for ciprofloxacin with the regression equation and R2 value.

“error bars are smaller than the symbol size”.

## Chapter 3

### Amoxicillin trihydrate

Amoxicillin was found in 1958 and was used for medicinal purposes in 1972. Amoxicillin is a broad-spectrum, semisynthetic aminopenicillin antibiotic with bactericidal activity.<sup>28</sup>

This medicine is used to treat infections caused by bacteria in different parts of the body. Amoxicillin trihydrate contain amoxicillin as the active ingredient which belongs to the penicillin family and is a  $\beta$ -lactam antibiotic.

#### 3.1 Structure

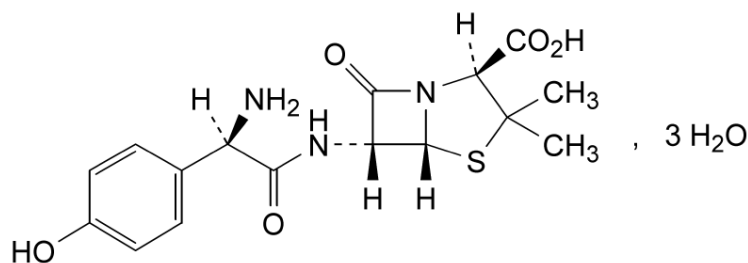


Figure 3.1: The structure of amoxicillin.<sup>28</sup>

#### 3.2 Chemical and physical properties

The amoxicillin trihydrate molecular formula is  $C_{16}H_{19}N_3O_5S \cdot 3H_2O$ , and the molecular weight is 419.45 g/mol. In terms of solubility, amoxicillin trihydrate is slightly water-soluble, very slightly ethanol-soluble. Capsules, tablets, and powder for oral suspension of amoxicillin are intended for oral administration.<sup>29</sup>

### **3.3 Materials and methods**

#### **3.3.1 Sampling**

A total of 57 blister packages of amoxicillin, representing 37 batch numbers containing 250 and 500 mg capsules were purchased from commercial outlets in eight countries. Twelve packages were obtained in the DRC (Kinshasa), 11 in Ghana (Accra and Tema), 21 in Sierra Leone (Freetown, Makeni and Kamakwie), seven in Haiti (Port-au-Prince), three in Ethiopia (Addis Ababa), and one each in Papua New Guinea (Port Moresby), India (New Delhi), and Canada (Ottawa, to serve as a control). Packages from Ghana and Sierra Leone were collected during a 2-week trip to those countries with the portable FT-IR. All samples were unexpired. A complete list of all packages and their origin can be found in Appendix A1, Table 1. Samples from the DRC were obtained from the central government depot, whereas the rest were purchased from private pharmacies.

#### **3.3.2 Sample preparation.**

Five capsules were removed from each blister pack (10 from the package from Canada) and analyzed separately (and reported as discrete data points for a total of 290 capsules measured). Capsule content weight was determined by calculating the difference between the total weight of the capsule and the empty capsule. For each capsule, two 30-mg aliquots of contents were dissolved in 50 mL of the mobile phase (see the following paragraphs) and filtered before analysis via ultra-high-performance liquid chromatography (UPLC)–ultraviolet (UV)/visible spectroscopy (UPLC-UV for short). The remainder of the capsule content was used for FT-IR analysis. Each capsule was subjected to duplicate measurements by UPLC-UV and triplicate

measurements by FT-IR, with the averages being reported in the figures and tables (see Appendix A.1).

### **3.3.3 UPLC-UV protocol.**

The UPLC-UV analysis was performed in accordance with the established pharmacopeia protocol<sup>29</sup> on an Agilent 1290 Infinity II system equipped with the following: the G7120A high-speed binary pump, the G7167B multisampler with a 25- $\mu$ L sample loop, the G7116B multicolumn thermostat, and the G7114B variable wavelength detector (VWD). Reagents were purchased from Sigma-Aldrich and acetonitrile was purchased from Fisher Scientific Canada. Amoxicillin trihydrate, pharmaceutical secondary standard, a certified reference material traceable to BP 19; PhEur A0900000; and USP 1031503 was purchased from Sigma-Aldrich. Standard calculations<sup>30</sup> were used to translate the HPLC pharmacopeia procedure to UPLC (which only changes mobile phase flow rate and column diameter). The mobile phase used was 0.2 M ACS-grade potassium phosphate monobasic at a pH of 5.0, adjusted with 2 M of ACS-grade sodium hydroxide, and UPLC-UV-quality acetonitrile at an isocratic ratio of 87:13. The flow rate for the mobile phase was 0.579 mL/minute. The stationary phase used was the Zorbax SB-C18 UPLC column with a column length of 0.05 m, an internal diameter of 2.1 mm, and a pore size of 1.8  $\mu$ m. An injection volume of 10  $\mu$ L was used and the VWD was set at 254 nm.<sup>29</sup>

Three aliquots of certified reference material-grade amoxicillin trihydrate (Sigma-Aldrich) was weighed in 15, 30, and 45 mg amounts and then dissolved in 50 mL of mobile phase and filtered. The standard was analyzed at the same time as the analyte sample to produce the external calibration curve for quantitation. The amount of amoxicillin in the analyzed aliquot interpolated from the calibration curve is converted to the relative amount of API in %w/w and

multiplied by the total weight of the capsule's contents.<sup>29</sup> A complete set of numerical results and their uncertainty can be found in Appendix A1, Table 3.

### **3.3.4 FT-IR protocol.**

In triplicate, approximately 30–50 mg from each capsule was placed on the FT-IR sampling crystal of an Agilent 4500a portable FT-IR equipped with a single-bounce attenuated total reflectance sampling accessory. Both background and sample analyses are measured at a resolution of 4  $\text{cm}^{-1}$ . One hundred and twenty-eight scans were performed over the spectral range of 4,000–650  $\text{cm}^{-1}$  for a total run time of 2 minutes.

The calibration curve of %w/w of amoxicillin (12 points varying between 0% and 84.6% of anhydrous amoxicillin) was prepared by varying the amount of amoxicillin trihydrate (see UPLC protocol for information on this standard) in a capsule and filling them to 594 mg with an excipient matrix as described in the literature.<sup>31</sup> Ten grams of excipient matrix was prepared by mixing 4.997 g of sodium dodecyl sulfate, 4.330 g of magnesium stearate, and 0.673 g of silicon dioxide. After that, all the excipients were ground with a mortar and pestle until it turns into a fine powder, approximately 3-5 minutes. All excipients were of ACS grade and purchased from Sigma-Aldrich. The standards were then run in triplicate and a partial least squares multiple linear regression calibration model was made using Agilent's MicroLab Expert with the area selected in the region of 1,800–1,150  $\text{cm}^{-1}$ . Examples of the IR spectrum of amoxicillin and the calibration mixtures are found in Figure 2.4 chapter 2 on IR calibration section. The software gives the relative percentage of weight to weight of the API. Multiplying this percentage by the total mass of the sample yields the total mass of the API. Dividing the total mass of API by the expected mass

from the package label results in the percentage API (%API) used in the figures. A complete set of numerical results and their uncertainty can be found in Appendix A1, Table 4.

### 3.4 Results and discussion

#### 3.4.1 Total dose mass

The simplest analysis performed on the capsules was to weigh them. This allowed for both the identification of outliers as well as the determination of the %API by FT-IR (see methodology). The results across all samples, plotted by country of origin, are shown in Figure 3.2 as the % relative standard deviation from the expected mass listed on the packaging. Individual results are listed in Excel spreadsheet format in Appendix A1, Table 2. All but five of the measurements fall within the allowable  $\pm 10\%$  of the listed mass, with a few exceptions. Notably, three of the capsules obtained from Haiti were significantly low. This points to poor quality control in the capsule filling process and leads to low values for the %API (see the following paragraphs).

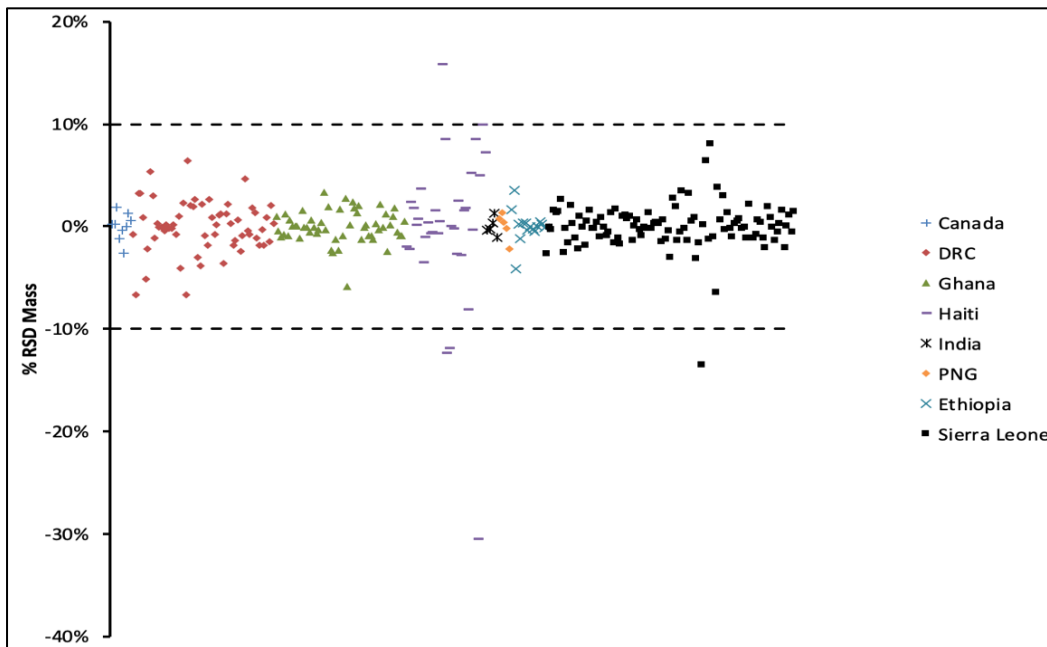


Figure 3.2: Mass results by countries.

### 3.4.2 UPLC-UV results

The results of the %API across all samples are summarized in Figure 3.3 as function of country of origin. Ninety-five percent of the capsules fell within the 90–110% limit for the %API, but 13 fell below that deemed acceptable. As expected, those capsules with very poor content masses by extension also had very low %API. Of particular concern were selected samples from Haiti, the DRC, Ghana, and Sierra Leone that fell well below 90% API, including one capsule from Haiti that contained only 65% API.

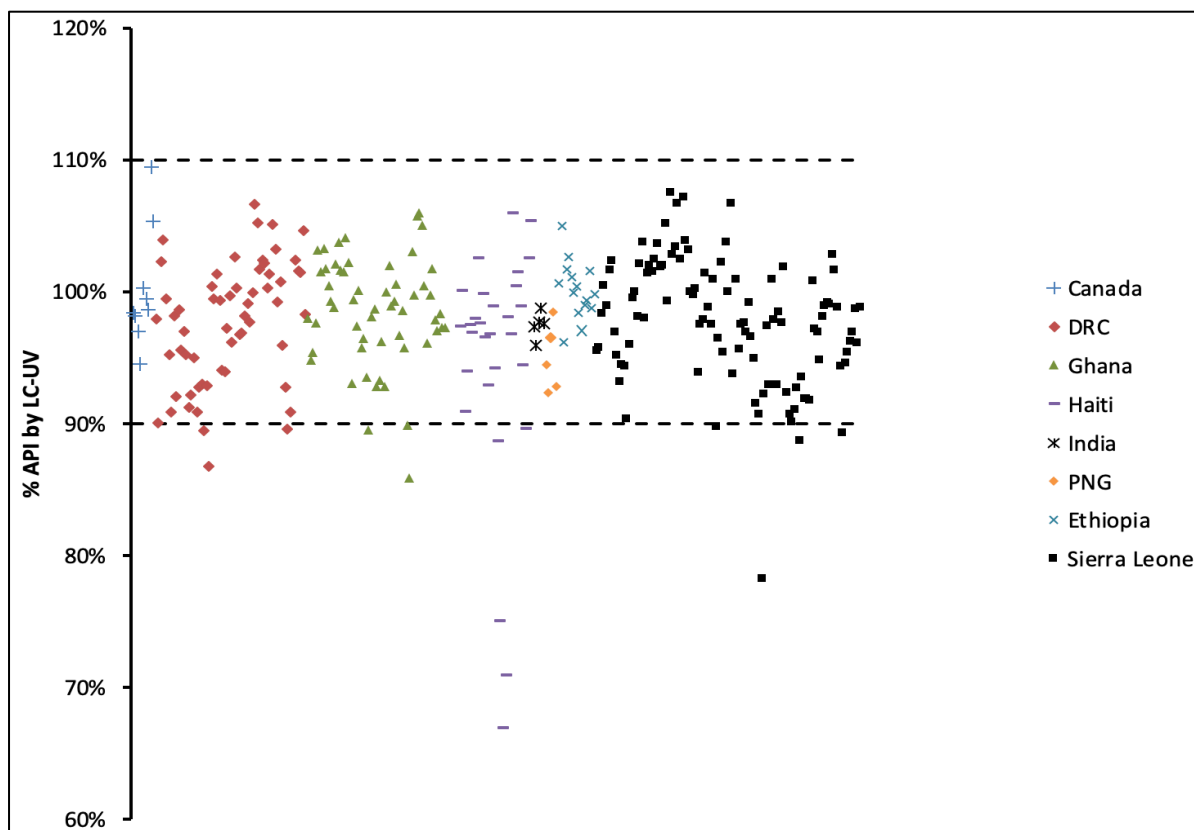


Figure 3.3: The LC-UV results for amoxicillin by countries.

### 3.4.3 FT-IR results

The results derived from the FT-IR protocol of the %API across all capsules are summarized in Figure 3.4 as a function of country of origin. As was seen in the UV results, most capsules (92%) fall inside the approved guidelines of 90–110% API. Eight percent of the capsules fell outside this range; however, all but four lie close to the 90% API cutoff.

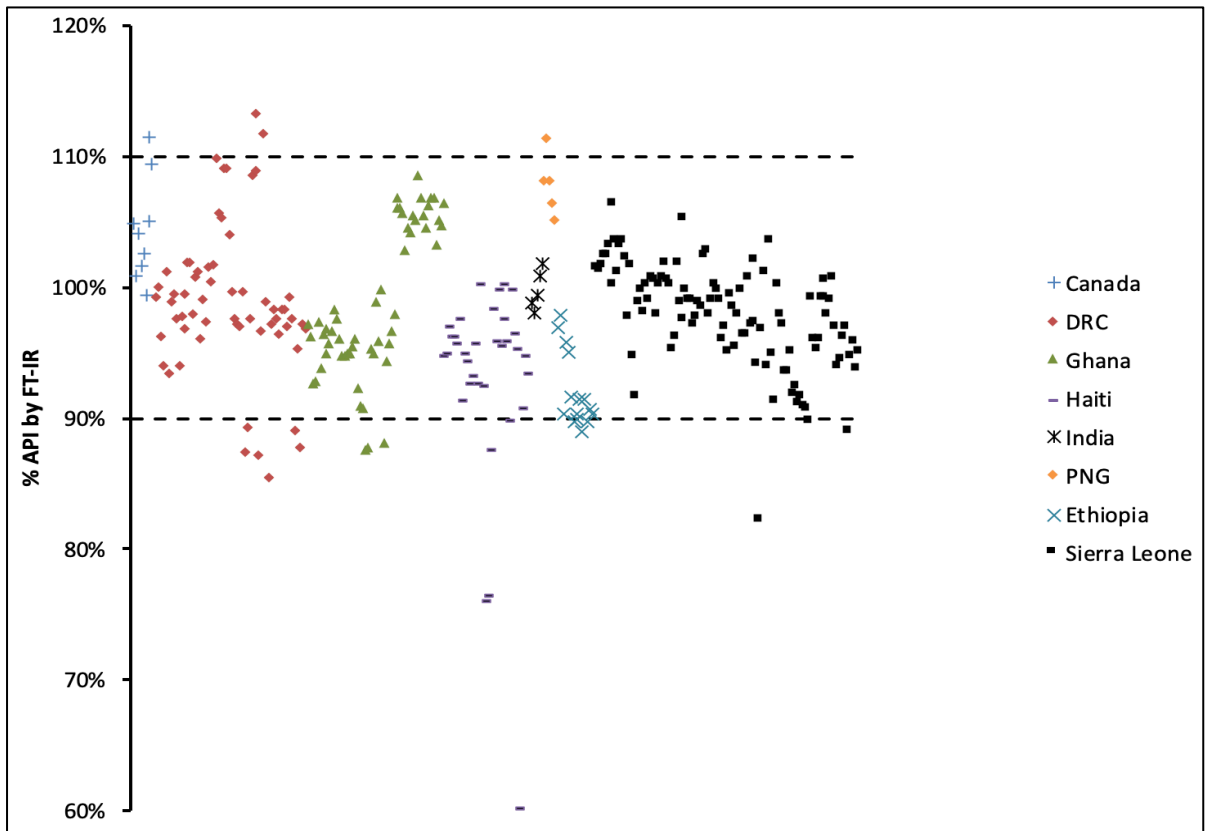


Figure 3.4: The FT-IR results for amoxicillin by countries.

### 3.4.4 UPLC vs FT-IR

Figure 3.5 displays the %API found for each capsule by the two techniques. The solid line represents the ideal 1:1 agreement between the two. There is generally good agreement between the two methods with the data clustering along the 1:1 line. The FT-IR predicts low %API values for the same capsules identified by LC-UV. In other words, the major outliers, and thus the capsules of concern, are identified by both techniques.

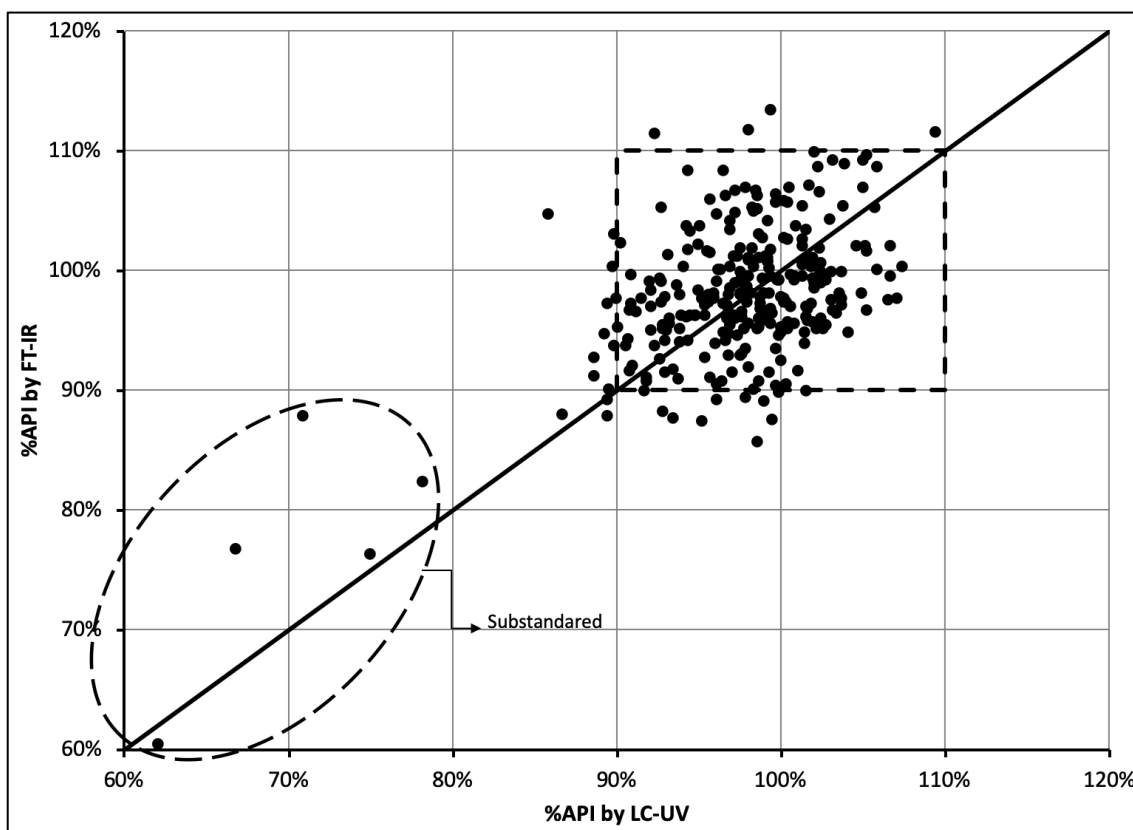


Figure 3.5: %API of amoxicillin by LC-UV vs. FT-IR.

## Chapter 4

### Ciprofloxacin Hydrochloride

Ciprofloxacin Hydrochloride is the hydrochloride salt form of ciprofloxacin, a fluoroquinolone related to nalidixic acid with antibacterial activity.<sup>32</sup>

This medication is used to treat a variety of bacterial infections. Ciprofloxacin belongs to a class of drugs called quinolone antibiotics.

#### 4.1 Structure

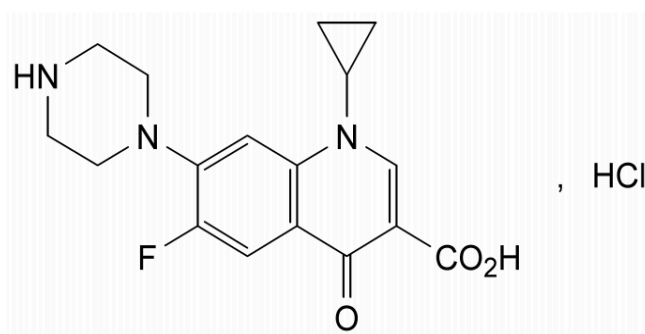


Figure 4.1: The structure of ciprofloxacin.<sup>32</sup>

#### 4.2 Chemical and physical properties

The molecular formula of ciprofloxacin hydrochloride is  $C_{17}H_{18}FN_3O_3 \cdot HCl$ , and the molecular weight is 367.8 g/mol. Ciprofloxacin hydrochloride is soluble in water, slightly soluble in methanol, very slightly soluble in ethanol, practically insoluble in acetone, in ethyl acetate and in methylene chloride.<sup>33</sup>

## **4.3 Materials and methods**

### **4.3.1 Sampling.**

A total of 55 blister packages of ciprofloxacin, representing 36 batch numbers containing 250 and 500 mg tablets were purchased from commercial outlets in nine countries. Two packages were obtained in the Democratic Republic of Congo (Kinshasa), 10 in Ghana (Accra and Tema, Atimpoku/volta Bridge), 12 in Sierra Leone (Freetown, Makeni and Kamakwie), 3 in Haiti (Port-au-Prince), 5 in Ethiopia (Addis Ababa) and 1 each in Papua New Guinea (Port Moresby), India (New Delhi), Indonesia (Jakarta) and Canada (Ottawa, to serve as a control). Packages from Ghana and Sierra Leone were collected during a two-week trip to those countries with the portable FT-IR. All samples were unexpired. A complete list of all packages and their origin can be found in Appendix A2, Table 1. Samples from the DRC were obtained from the central government depot, while the rest were purchased from private pharmacies.

### **4.3.2 Sample preparation.**

Five tablets were removed from each blister pack (10 from the package from Canada) and analyzed separately (and reported as discrete data points for a total of 280 tablets of ciprofloxacin measured). For each tablet, two 30 mg aliquots of contents were dissolved in 50 mL of the mobile phase (see the following paragraph) and filtered before analysis via UPLC-UV. The remainder of the tablet was used for FT-IR analysis. Each tablet was subjected to duplicate measurements by UPLC-UV and triplicate measurements by FT-IR, with the averages being reported in the figures and tables (see Appendix A2).

### 4.3.3 UPLC protocol.

The UPLC-UV analysis was performed in accordance with the established pharmacopeia protocol<sup>33</sup> on an Agilent 1290 Infinity II system equipped with the following: the G7120A high-speed binary pump, the G7167B multisampler with a 25- $\mu$ L sample loop, the G7116B multicolumn thermostat, and the G7114B variable wavelength detector (VWD). Reagents were purchased from Sigma-Aldrich and acetonitrile was purchased from Fisher Scientific Canada. Ciprofloxacin hydrochloride, pharmaceutical secondary standard, and USP 1031503 was purchased from Sigma-Aldrich. Standard calculations<sup>30</sup> were used to translate the HPLC pharmacopeia procedure to UPLC (which only changes mobile phase flow rate and column diameter). The mobile phase used was 2.45 g/L phosphoric acid at pH of 3.0, adjusted with 2M of ACS grade sodium hydroxide, and UPLC-UV quality acetonitrile at an isocratic ratio of 87:13. The flow rate for the mobile phase was 0.87 ml/min. The stationary phase used was the Zorbax SB-C18 UPLC column with a column length of 0.05 m, an internal diameter of 2.1 mm and a pore size of 1.8  $\mu$ m. An injection volume of 10  $\mu$ L was used and the VWD was set at 278 nm<sup>33</sup>.

Three aliquots of certified reference material grade ciprofloxacin (Sigma-Aldrich) were weighed in 10, 25 and 40 mg amounts then dissolved in 50 mL of mobile phase and filtered. The standard was analyzed at the same time as the analyte sample to produce the external calibration curve for quantitation. The amount of ciprofloxacin in the analyzed aliquot interpolated from the calibration curve is converted to the relative amount of API in %w/w and multiplied by the total weight of the capsule's and tablet's contents.<sup>33</sup> A complete set of numerical results and their uncertainty can be found in Appendix A2, Table 3.

#### 4.3.4 FT-IR Protocol.

In triplicate, approximately 30 to 50 mg from each tablet was placed on the FT-IR sampling crystal of an Agilent 4500a portable FT-IR equipped with a single-bounce attenuated total reflectance (ATR) sampling accessory. Both background and sample analyses are measured at a resolution of  $4\text{ cm}^{-1}$ . 128 scans were done over the spectral range of  $4000 - 650\text{ cm}^{-1}$  for a total run time of 2 minutes.

The calibration curve of % w/w of ciprofloxacin (11 points varying between 0 and 88.74% of anhydrous ciprofloxacin) was prepared by varying the amount of ciprofloxacin hydrochloride in a capsule and filling them to 500 mg with an excipient matrix as described in the literature<sup>34</sup>. Five grams of excipient matrix was prepared by mixing 821.4 mg of erospovidon, 2181.5 mg of sodium starch glycolate, 259.6 mg of povidone, 1483.0 mg of cellulose, 165.5 mg of magnesium stearate, and 95.8 mg silicon dioxide. After that, all the excipients were ground with a mortar and pestle until it turns into a fine powder, approximately 3-5 minutes. All excipients were of ACS grade and purchased from Sigma-Aldrich. The standards were run in triplicate and partial least squares (PLS1) multiple linear regression calibration models were made using Agilent's MicroLab Expert with the area selected in the region of  $1063.133-1768.786\text{ cm}^{-1}$ ,  $2539.604-2803.991\text{ cm}^{-1}$  and  $3463.096-3593.428\text{ cm}^{-1}$ . The software gives the relative percentage of weight to weight of the API. Multiplying this percentage by the total mass of the sample yields the total mass of the API. Dividing the total mass of API by the expected mass from the package label results in the API (%API) used in the figures. A complete set of numerical results and their uncertainty can be found in Appendix A2, Table 4.

## 4.4 Results and discussion

### 4.4.1 Total dose mass.

The simplest analysis performed on the tablets was to weigh them. This allowed for both the identification of outliers as well as the determination of the %API by FT-IR (see methodology). The results across all samples, plotted by country of origin, are shown in Figure 4.2 as the % relative standard deviation from the expected mass listed on the packaging. Individual results are listed in Excel spreadsheet format in Appendix A2, Table 2. All the measurements fall within the allowable  $\pm 10\%$  of the listed mass.

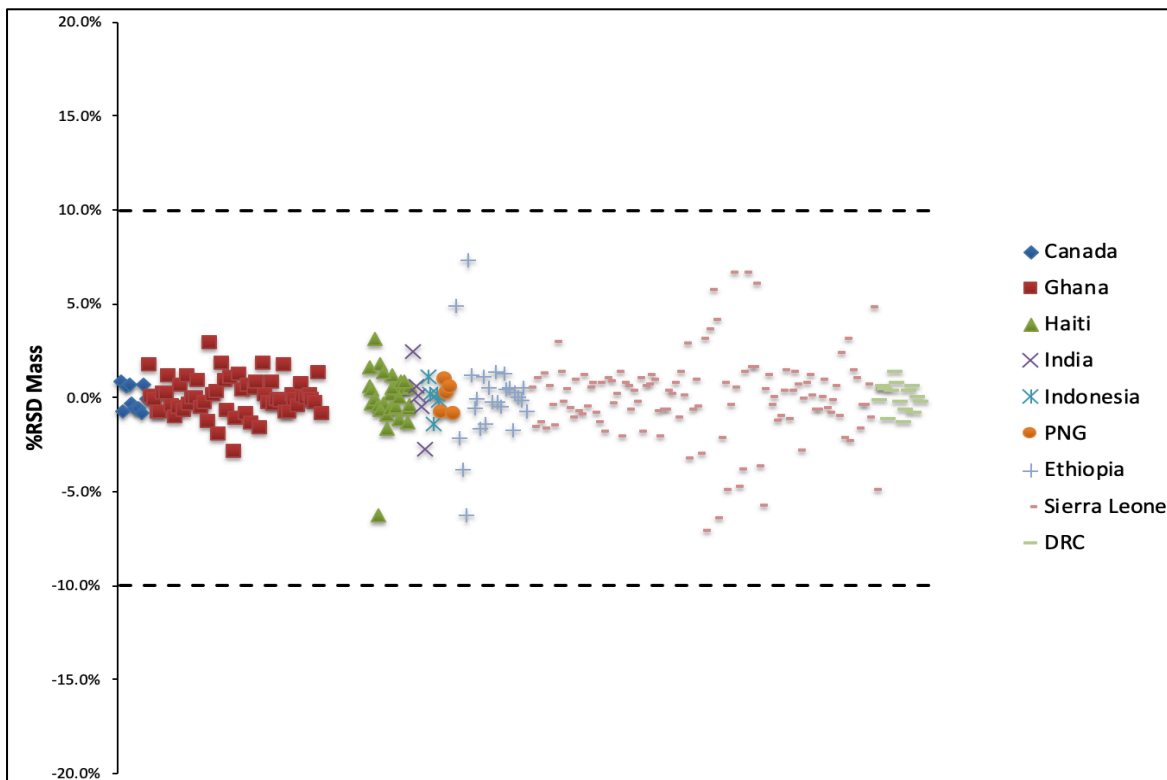


Figure 4.2: The mass results for ciprofloxacin by countries.

#### 4.4.2 UPLC-UV results.

The results of the %API across all samples are summarized in Figure 4.3 as a function of country of origin. The majority of the tablets fell within the 90–110% limit for the %API, but fourteen fell up and below that deemed acceptable. Although all the tablets mass fell within the range  $\pm 10\%$ , five tablets contained more than the allowed amount of API and the remaining nine tablets had an insufficient amount of the active pharmaceutical ingredients.

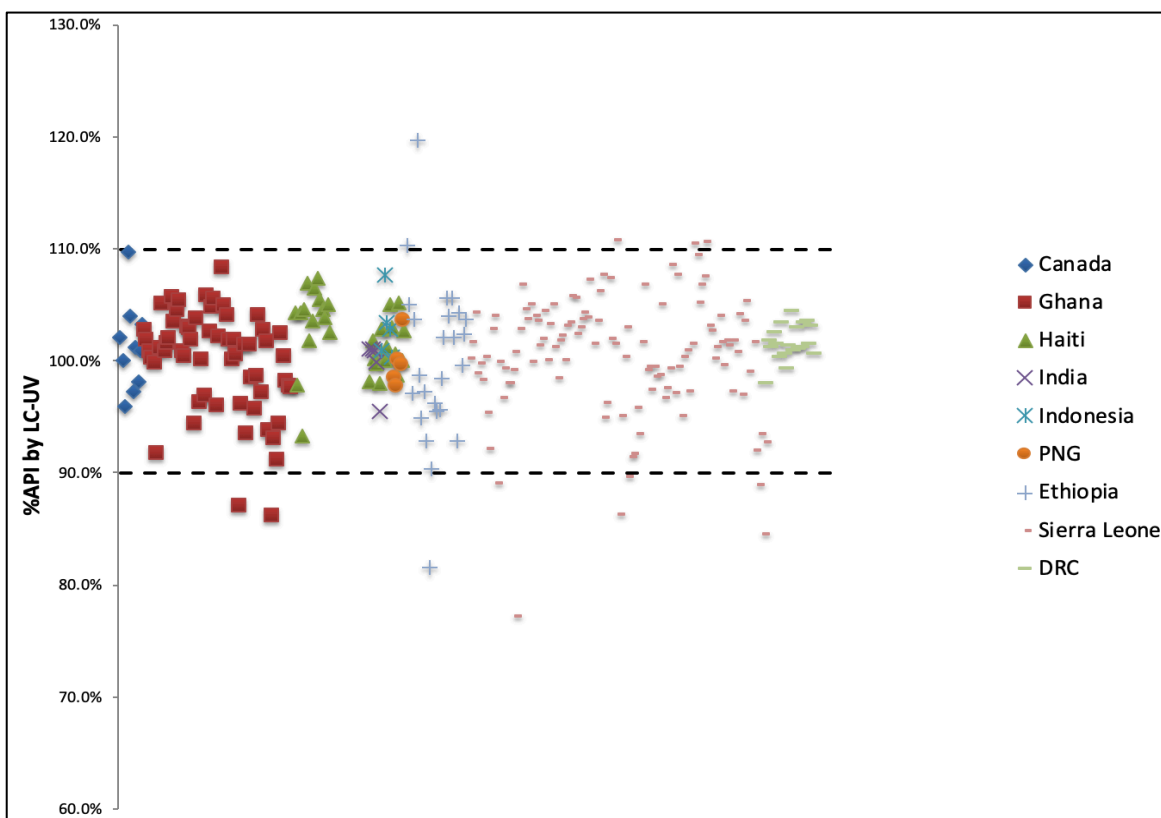


Figure 4.3: The LC-UV results for ciprofloxacin by countries.

### 4.4.3 FT-IR results.

The results derived from the FT-IR protocol of the %API across all tablets are summarized in Figure 4.4 as a function of the country of origin. 236 out of 280 tablets fall inside the approved guidelines of 90–110% API. Forty-four of the tablets fell outside this range. Thirty-four of the tablets that fell outside the acceptable range fell down 90%, and five of them lie very close to the 90% API cutoff. The remaining ten tablets fell close to 110%.

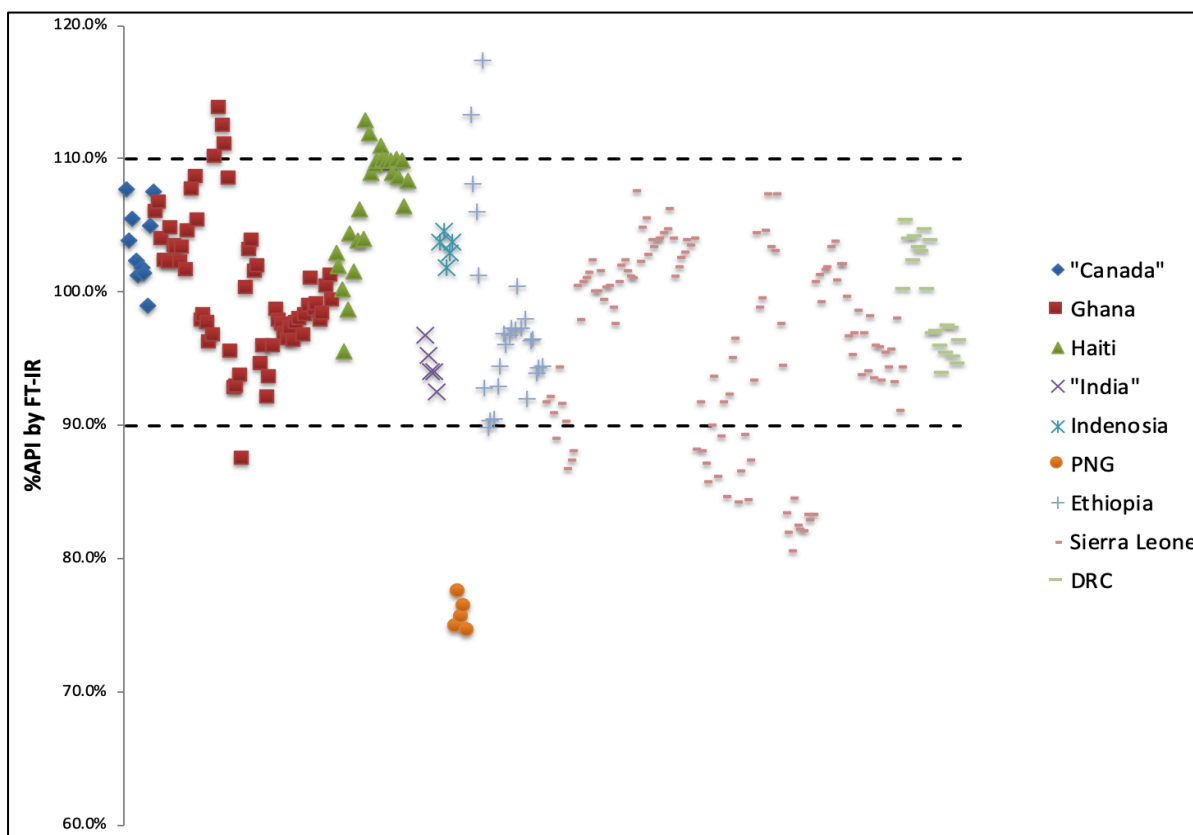


Figure 4.4: The FT-IR results for ciprofloxacin by countries.

#### 4.4.4 UPLC vs FT-IR

Figure 4.5 displays the %API found for each capsule by the two techniques. The solid line represents the ideal 1:1 agreement between the two. There is generally good agreement between the two methods with the data clustering along with the 1:1 line. The FT-IR predicts low %API values for the same tablets identified by LC-UV. In other words, the major outliers, and thus the capsules of concern, are identified by both techniques.

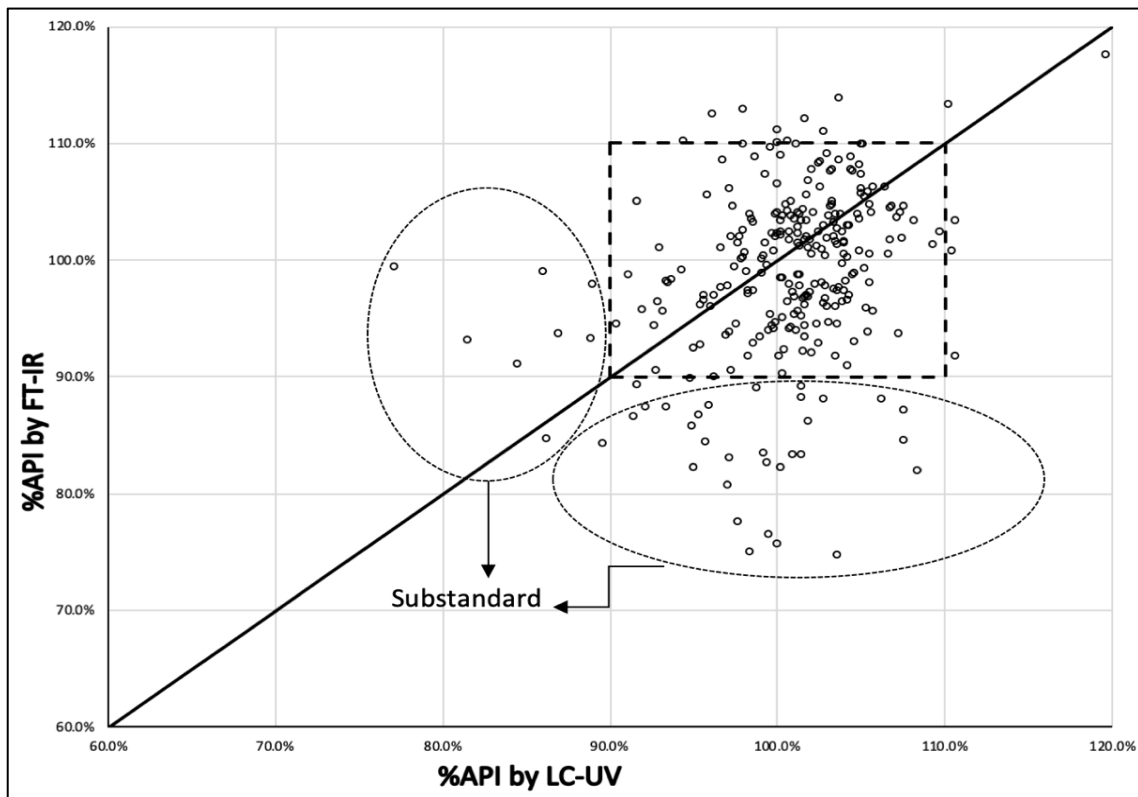


Figure 4.5: %API of ciprofloxacin by LC-UV vs. FT-IR.

## Chapter 5

### Doxycycline hyclate

Doxycycline hyclate is the hyclate salt form of doxycycline, a synthetic, broad-spectrum tetracycline antibiotic exhibiting antimicrobial activity. Doxycycline can be used either by mouth or by injection into a vein.<sup>35</sup>

#### 5.1 Structure

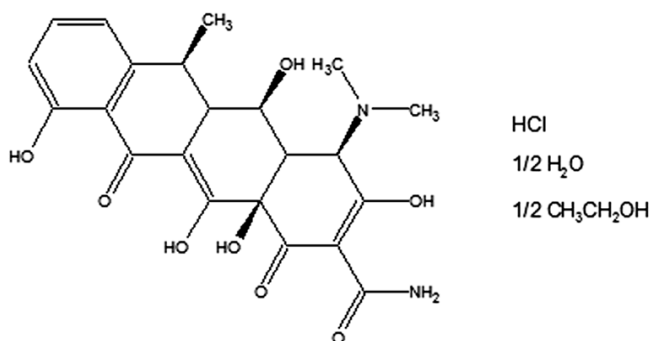


Figure 5.1: The structure of doxycycline.<sup>34</sup>

#### 5.2 Chemical and physical properties

The formula of the molecular of doxycycline hyclate is C<sub>22</sub>H<sub>24</sub>N<sub>2</sub>O<sub>8</sub>, HCL,0.5 C<sub>2</sub>H<sub>5</sub>OH,0.5 H<sub>2</sub>O, and the weight of the molecular is 512.94 g/mol. Doxycycline hyclate is freely soluble in water and methanol, sparingly soluble in ethanol.<sup>35</sup>

## **5.3 Materials and methods**

### **5.3.1 Sampling.**

A total of 17 blister packages of doxycycline, representing 10 batch numbers containing 100 mg tablets and capsules were purchased from commercial outlets in 6 countries. 11 packages were obtained in Ghana (Accra and Tema, Atimpoku/Volta Bridge), 2 in Sierra Leone (Freetown, Makeni and Kamakwie), and one each in Papua New Guinea (Port Moresby), India (New Delhi), in Ethiopia (Addis Ababa), and Canada (Ottawa, to serve as a control). Packages from Ghana and Sierra Leone were collected during a two-week trip to those countries with the portable FT-IR. All samples were unexpired and purchased from private pharmacies. A complete list of all packages and their origin can be found in Appendix A3, Table 1.

### **5.3.2 Sample preparation.**

Five capsules and tablets were removed (10 from the package from Canada) and analyzed separately (and reported as discrete data points for a total of 42 of tablets and capsules of doxycycline measured). Capsule content weight was determined by calculating the difference between the total weight of the capsule and the empty capsule. The samples were analyzed first in the FT-IR then the remainder capsule content was run via UPLC-UV. For each tablet and capsule, two 6.2 mg aliquots of contents were dissolved in 10 mL of the mobile phase (see the following paragraph) and filtered before analysis via UPLC-UV. Each tablet and capsule were subjected to duplicate measurements by UPLC-UV and triplicate measurements by FT-IR, with the averages being reported in the figures and tables (see Appendix A3).

### 5.3.3 UPLC protocol.

The UPLC-UV analysis was performed in accordance with the established pharmacopeia protocol<sup>35</sup> on an Agilent 1290 Infinity II system equipped with the following: the G7120A high-speed binary pump, the G7167B multisampler with a 25- $\mu$ L sample loop, the G7116B multicolumn thermostat, and the G7114B variable wavelength detector (VWD). Reagents were purchased from Sigma-Aldrich and acetonitrile was purchased from Fisher Scientific Canada. Doxycycline hyclate, pharmaceutical secondary standard, and USP 1031503 was purchased from Sigma-Aldrich. Standard calculations<sup>30</sup> were used to translate the HPLC pharmacopeia procedure to UPLC (which only changes mobile phase flow rate and column diameter). The mobile phase used was water with 0.1% of trifluoroacetic acid (TFA), and acetonitrile adjusted with 0.1% of TFA. The ratio was 60:40. The flow rate for the mobile phase was 0.58 ml/min. The stationary phase used was the Zorbax SB-C18 UPLC column with a column length of 0.05m, an internal diameter of 2.1 mm and a pore size of 18  $\mu$ m. An injection volume of 0.8  $\mu$ L was used and the VWD was set at 360 nm.<sup>35</sup>

One aliquot of certified reference material grade doxycycline (Sigma-Aldrich) was weighed in 50 mg amount then dissolved in 50 ml of the mobile phase and filtered then three dilutions were taken in 0.5%, 0.1%, and 0.05%. The standard was analyzed at the same time as the analyte sample to produce the external calibration curve for quantitation. The amount of doxycycline in the analyzed aliquot interpolated from the calibration curve is converted to the relative amount of API in %w/w and multiplied by the total weight of the capsule's and tablet's contents.<sup>35</sup> A complete set of numerical results and their uncertainty can be found in Appendix A3, Table 3.

### 5.3.4 FT-IR protocol.

In triplicate, approximately 20 to 30 mg from each capsule of doxycycline was placed on the FT-IR sampling crystal of an Agilent 4500a portable FT-IR equipped with a single bounce attenuated total reflectance (ATR) sampling accessory. Both background and sample analyses are measured at a resolution of  $4\text{ cm}^{-1}$ . 128 scans were done over the spectral range of 4000 -650  $\text{cm}^{-1}$  for a total run time of 2 minutes.

The calibration curve of %w/w of doxycycline (11 points varying between 0 and 81.55% of hyclate doxycycline) was prepared by varying the amount of doxycycline hyclate in a capsule and filling them to the same amount with an excipient matrix. 16.600 grams of excipient matrix was prepared by mixing 13 grams of microcrystalline cellulose (Avicel PH 102), 2 grams of Starch (cornstarch dried), 300 mg of sodium lauryl sulphate, 300 mg of sodium silicon dioxide (Aerosil 200), and 1-gram magnesium stearate. After that, all the excipients were ground with a mortar and pestle until it turns into a fine powder, approximately 3-5 minutes. All excipients were of ACS grade and purchased from Sigma-Aldrich. The standards were then run in triplicate and partial least squares (PLS1) multiple linear regression calibration models were made using Grams IQ with the area selected in the region of 1735.2-1489.5  $\text{cm}^{-1}$ . The software gives the relative percentage of weight to weight of the API. Multiplying this percentage by the total mass of the sample yields the total mass of the API. Dividing the total mass of API by the expected mass from the package label results in the %API used in the figures. A complete set of numerical results and their uncertainty can be found in Appendix A3, Table 4.

## 5.4 Results and discussion

### 5.4.1 Total dose mass.

The simplest analysis performed on the tablets was to weigh them. This allowed for both the identification of outliers as well as the determination of the %API by FT-IR (see methodology). The results across all samples, plotted by country of origin, are shown in Figure 5.2 as the % relative standard deviation from the expected mass listed on the packaging. Individual results are listed in Excel spreadsheet format in Appendix A3 Table1. All the measurements fall within the allowable  $\pm 10\%$  of the listed mass.

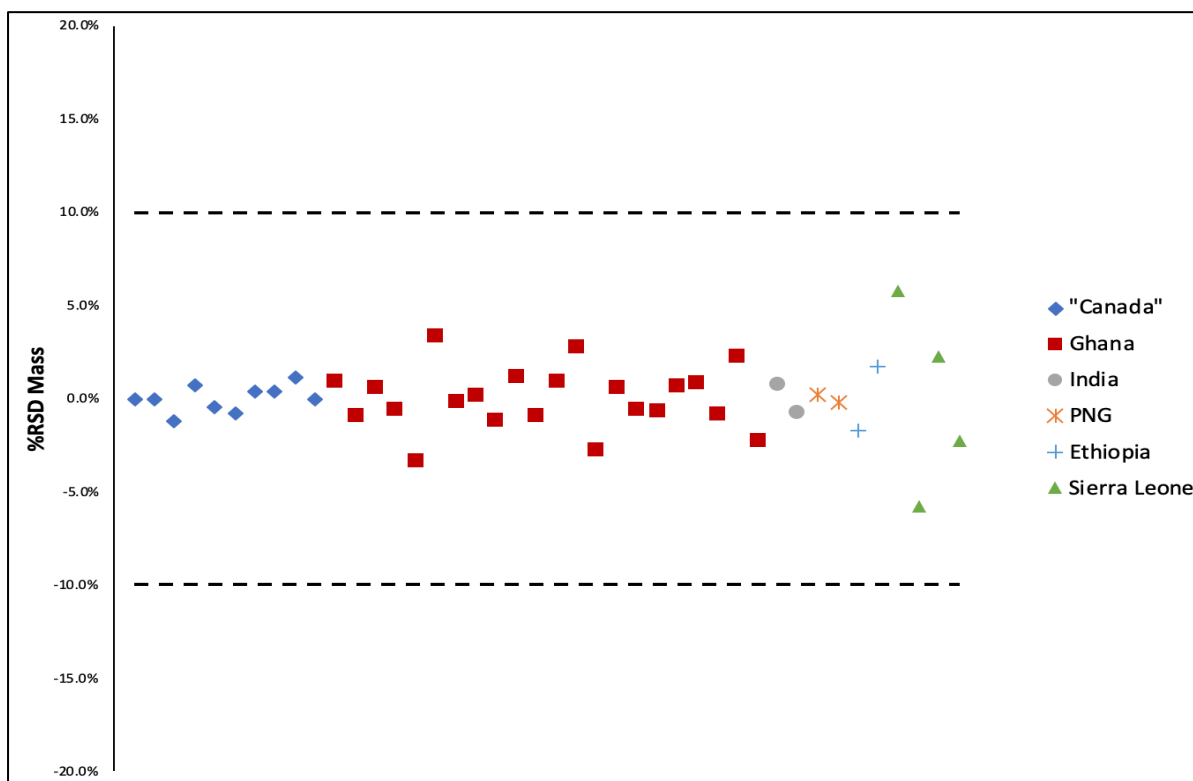


Figure 5.2: The mass results for doxycycline by countries.

### 5.4.2 UPLC-UV results.

The results of the %API across all samples are summarized in Figure 5.3 as a function of country of origin. More than half of the capsules fell out the satisfactory range of the active pharmaceutical ingredients (90% - 110%). One sample of the 28 pills that lie out of 90- 110% is close to 110%, and five located in the range of eighty.

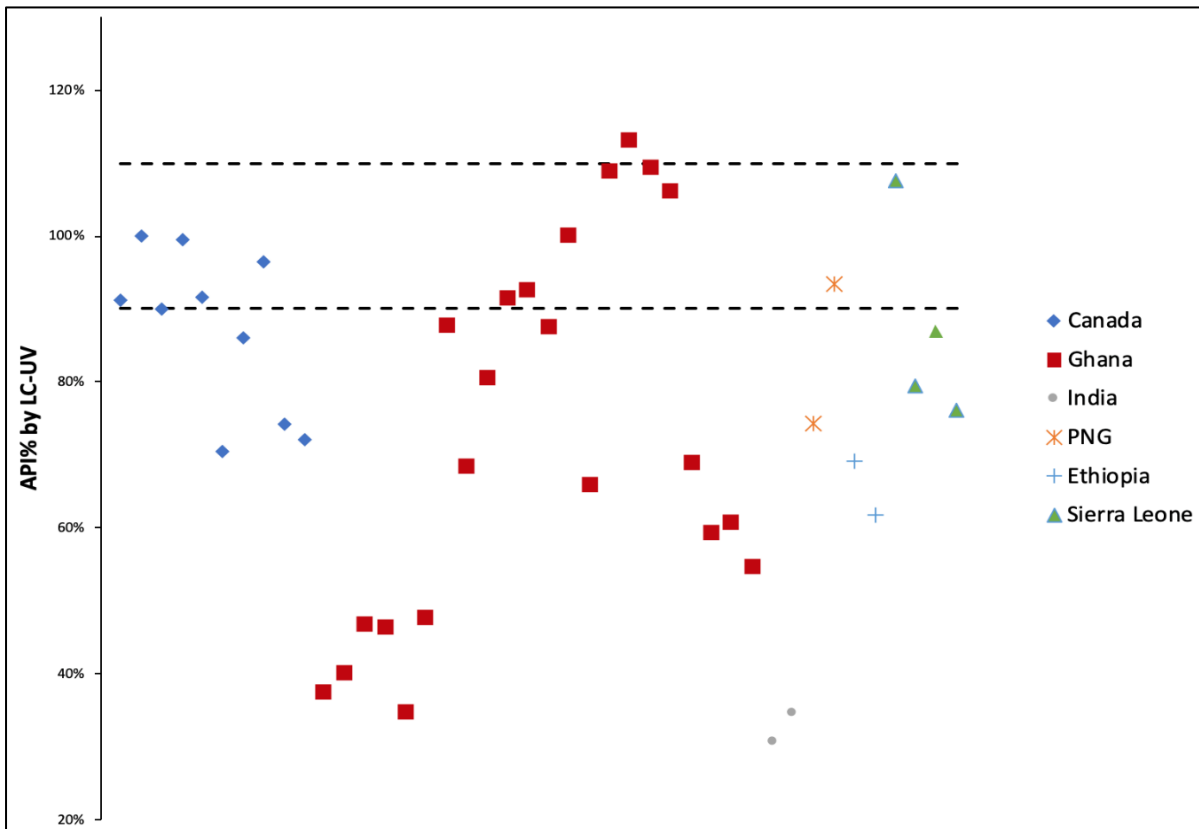


Figure 5.3: The LC-UV results for doxycycline by countries.

### 5.4.3 FT-IR results.

The results derived from the FT-IR protocol of the %API across all tablets are summarized in Figure 5.4 as a function of the country of origin. 24 out of 42 tablets fall inside the approved limit of 90–110% active pharmaceutical ingredients and the rest lie outside this range.

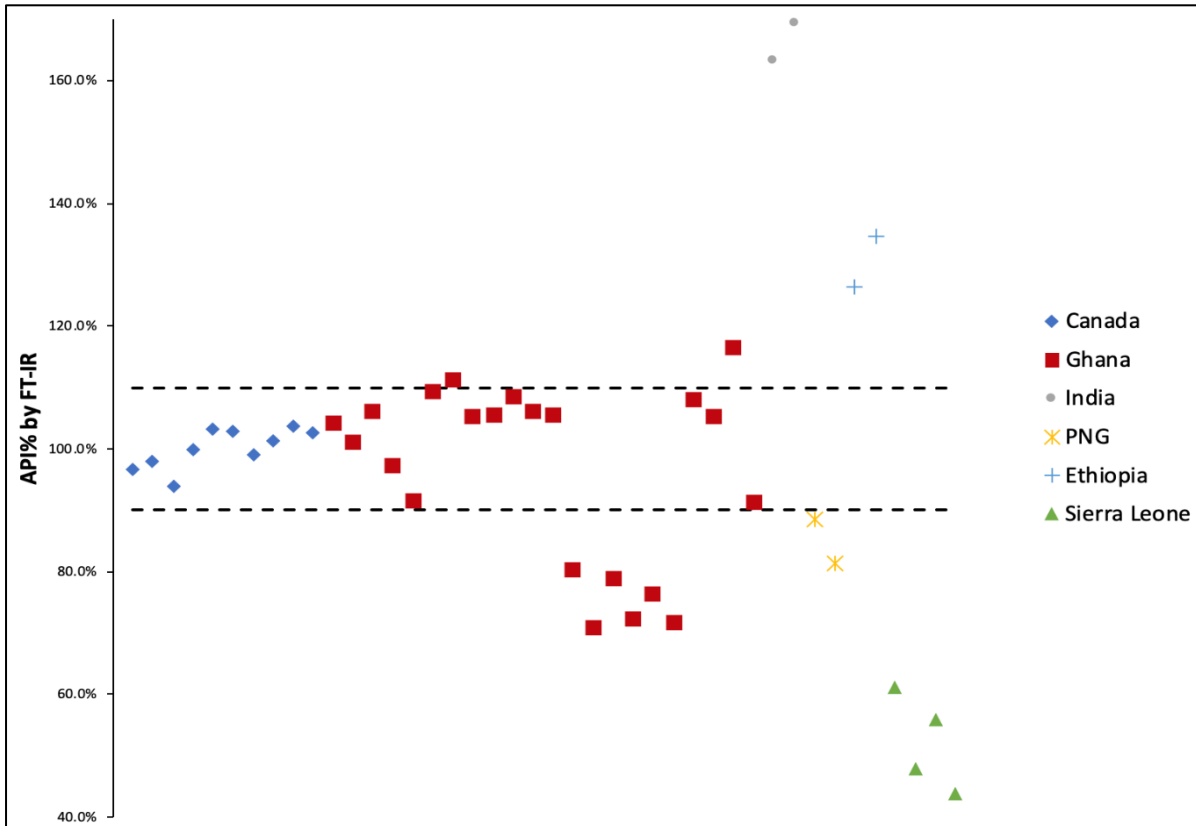


Figure 5.4: The FT-IR results for doxycycline by countries.

#### 5.4.4 UPLC vs FT-IR

Figure 5.5 displays the %API found for each capsule by the two techniques. The solid line represents the ideal 1:1 agreement between the two. There is not a good agreement between the two methods with the data clustering along with the 1:1 line. When FT-IR predicts low %API values, the UV gives the opposite values. Noticeably, samples 0004 and 0007 have the most significant mass, the least LC-UV results, and the highest FT-IR results.

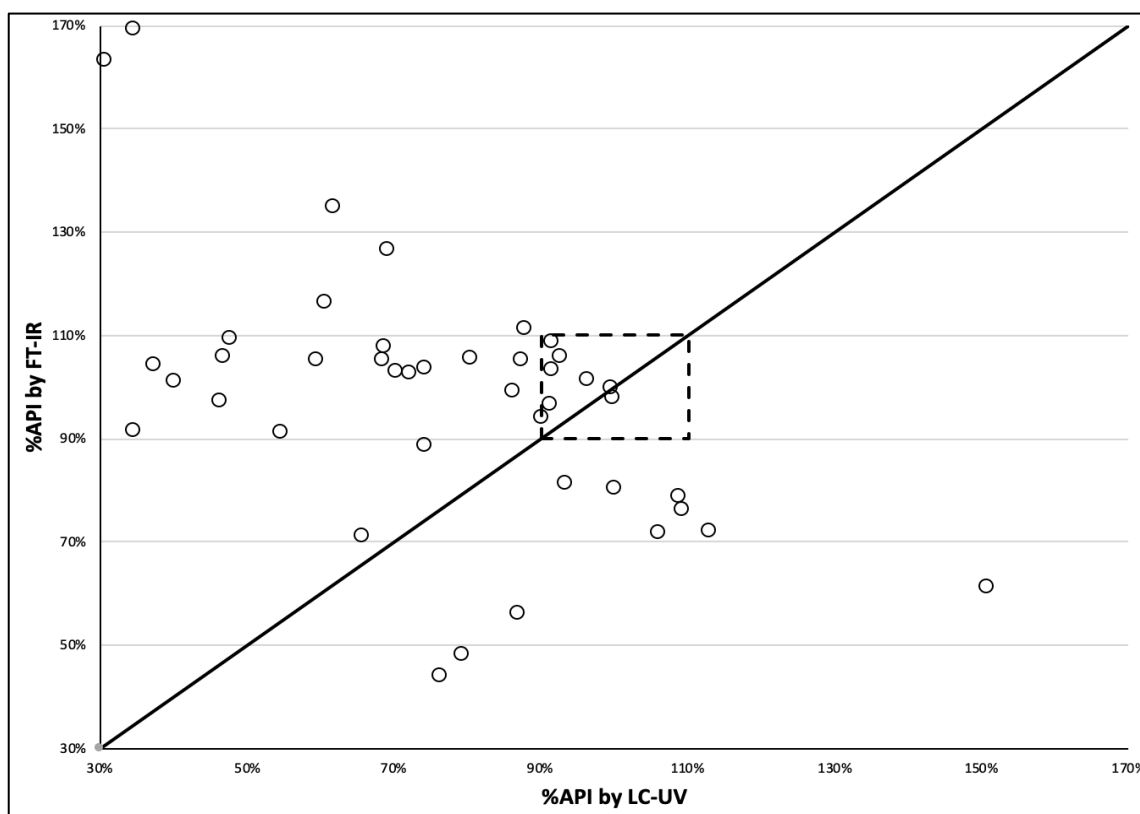


Figure 5.5: %API of doxycycline by LC-UV vs. FT-IR

The disagreement between both techniques, in this case, might be due to several reasons. Usually, we run the samples in the LC-UV then by the FT-IR, but in the doxycycline case, we did the opposite. Storing the content of the capsules after grinding them for eight months before

running them by the LC-UV could be a reason to change the chemical properties of the antibiotic. In addition, perhaps the reason is that there are limits to the capabilities of the Fourier transform IR spectrometer. One of those limitations is the masking effect. Masking effect happens in drug studies when we are analyzing a mixture of compounds. When an excipient and active pharmaceutical ingredient have dipole moments, they can absorb IR at similar wavelengths. The excipient compound masks the signal (peak) of our actual active drug compound that we want to analyze. As a result, the disagreement between the two methods LC-UV and FT-IR is significant.

## Chapter 6

### Conclusions

Poor-quality medicines present a serious public health problem, particularly in emerging economies and developing countries, and may have a significant impact on the national clinical and economic burden. Substandard medicines are widespread and represent a threat to health because they can inadvertently lead to healthcare failures, such as antibiotic resistance and the spread of disease within a community, as well as death or additional illness in individuals.

Regarding drug quality, 13 of 290, 14 of 280, and 28 of 42 individual capsules and tablets of amoxicillin, ciprofloxacin, and doxycycline respectively were found to be substandard with total API lying outside the acceptable range of 90–110%. The FT-IR reliably identified these outliers and was found to yield results in good agreement, except for the doxycycline, with the established pharmacopeia UPLC-UV protocol. Matrix effects were clearly identifiable in the FT-IR since the entire IR spectrum is being acquired, rather than a single wavelength. This avoids false readings from entering into the results. It is possible to modify the spectral window used in the calibration and analyses after the fact, without having to rerun samples, to account for small changes in excipient composition. This can be performed quickly on-site by the field technician using the instrument software. When calibration needs to be updated with new excipients, previously obtained IR data can simply be reloaded and checked against the new calibration (perhaps performed in a laboratory), without rerunning the original samples. This avoids the necessity of prolonged sample storage which may, by necessity, be in suboptimum conditions.

To conclude, the field portable FT-IR may be suitable to intercept substandard antibiotics in developing countries where more sophisticated techniques are not available. The benefits of the FT-IR come from its relatively low cost, its portability, simplicity of use, and rapid analysis time.

## Bibliography

1. Höllein L, Kaale E, Mwalwisi YH, Schulze MH, Holzgrabe U. Routine quality control of medicines in developing countries: Analytical challenges, regulatory infrastructures and the prevalence of counterfeit medicines in Tanzania. *TrAC - Trends Anal Chem.* 2016;76:60-70.
2. WHO. *Substandard / Spurious / Falsely-Labelled / Falsified / Counterfeit Medical Products.* Geneva, Switzerland; 2012.
3. Interpol. *2004–2014—Ten Years of Combating Pharmaceutical Crime: Review and Prospects, Dublin, Ireland 19–20 November 2014.* Lyon, France; 2014.
4. Pezzola A, Sweet CM. Global pharmaceutical regulation: The challenge of integration for developing states. *Global Health.* 2016;12:85.
5. Nickerson JW, Attaran A, Westerberg BD, Curtis S, Overton S, Mayer P. Fatal bacterial meningitis possibly associated with substandard ceftriaxone — Uganda, 2013. *Morb Mortal Wkly Rep.* 2016;64:1375-1377.
6. Mumphansha H, Nickerson JW, Attaran A, et al. An Analysis of Substandard Propofol Detected in Use in Zambian Anesthesia. *Anesth Analg.* 2017;125:616-619.
7. Nayyar GML, Breman JG, Newton PN, Herrington J. Poor-quality antimalarial drugs in southeast Asia and sub-Saharan Africa. *Lancet Infect Dis.* 2012;12:488-496.
8. Nayyar GML, Breman JG, Herrington JE. The global pandemic of falsified medicines: laboratory and field innovations and policy perspectives. *Am J Trop Med Hyg.* 2015;92:2-7.
9. Senior V. Antimicrobial resistance: What does medicine quality have to do with it? 2015.

10. Hajjou M, Krech L, Lane-Barlow C, et al. Monitoring the quality of medicines: results from Africa, Asia, and South America. *Am J Trop Med Hyg.* 2015;92:68-74.
11. Bate R, Coticelli P, Tren R, Attaran A. Antimalarial drug quality in the most severely malarious parts of Africa - A six country study. *PLoS One.* 2008;3:3-5.
12. Kaur H, Goodman C, Thompson E, et al. A nationwide survey of the quality of antimalarials in retail outlets in Tanzania. *PLoS One.* 2008;3:1-7.
13. Martino R, Malet-Martino M, Gilard V, Balayssac S. Counterfeit drugs: Analytical techniques for their identification. *Anal Bioanal Chem.* 2010;398:77-92.
14. Jamrógiewicz M. Application of the near-infrared spectroscopy in the pharmaceutical technology. *J Pharm Biomed Anal.* 2012;66:1-10.
15. Been F, Roggo Y, Degardin K, Esseiva P, Margot P. Profiling of counterfeit medicines by vibrational spectroscopy. *Forensic Sci Int.* 2011;211:83-100.
16. Sacré PY, Deconinck E, De Beer T, et al. Comparison and combination of spectroscopic techniques for the detection of counterfeit medicines. *J Pharm Biomed Anal.* 2010;53:445-453.
17. Bate R, Tren R, Hess K, Mooney L, Porter K. Pilot study comparing technologies to test for substandard drugs in field settings. *African J Pharm Pharmacol.* 2009;3:165-170.
18. Mbinze JK, Sacré PY, Yemoa A, et al. Development, validation and comparison of NIR and Raman methods for the identification and assay of poor-quality oral quinine drops. *J Pharm Biomed Anal.* 2015;111:21-27.
19. Said MM, Gibbons S, Moffat AC, Zloh M. Near-infrared spectroscopy (NIRS) and chemometric analysis of Malaysian and UK paracetamol tablets: A spectral database

- study. *Int J Pharm.* 2011;415:102-109.
20. Pavia DL, Lampman GM, Kriz GS, Vyvyan JR. INFRARED SPECTROSCOPY. In: *Introduction to Spectroscopy*. Nelson Education, 2014; 2013:15-28.
  21. Bunaciu AA, Aboul-Enein HY, Fleschin S. Application of fourier transform infrared spectrophotometry in pharmaceutical drugs analysis. *Appl Spectrosc Rev.* 2010;45:206-219.
  22. Smith BC. *Fundamentals of Fourier Transform Infrared Spectroscopy*. New York, NY: CRC Press; 2011.
  23. PerkinElmer. FT-IR Spectroscopy Attenuated Total Reflectance (ATR). PerkinElmer Life and Analytical Sciences. [https://cmdis.rpi.edu/sites/default/files/ATR\\_FTIR.pdf](https://cmdis.rpi.edu/sites/default/files/ATR_FTIR.pdf). Published 2005.
  24. Tobias RD. An introduction to partial least squares regression. *SAS Conf Proc SAS Users Gr Int 20 (SUGI 20)*. 1995:2-5. doi:<http://support.sas.com/techsup/technote/ts509.pdf>
  25. Kumar A, Saini G, Nair A, Sharma R. UPLC: A preeminent technique in pharmaceutical analysis. *Acta Pol Pharm - Drug Res.* 2012;69:371-380.
  26. Dong MW. *Modern HPLC for Practicing Scientists*. New Jersey: John Wiley & Sons, Inc., Hoboken; 2006.
  27. Malviya R, Bansal V, Pal OP, Sharma PK. High performance liquid chromatography: A short review. *J Glob Pharma Technol.* 2010;2:22-26.
  28. Amoxicillin trihydrate. National Center for Biotechnology Information. PubChem Database. <https://pubchem.ncbi.nlm.nih.gov/compound/Amoxicillin-trihydrate>. Accessed November 13, 2019.

29. British Pharmacopoeia Commission. Amoxicillin trihydrate (Amoxicillinum trihydricum). International Pharmacopoeia 2009. [http://www.uspbpep.com/ep60/amoxicillin trihydrate 0260e.pdf](http://www.uspbpep.com/ep60/amoxicillin-trihydrate-0260e.pdf). Published 2009. Accessed October 1, 2017.
30. Sigma Aldrich. HPLC Method Transfer Calculator. <https://www.sigmaaldrich.com/analytical-chromatography/hplc/method-transfer-calculator.html>. Published 2018.
31. Niazi SK. *Handbook of Pharmaceutical Manufacturing Formulations: Uncompressed Solid Products*. New York, NY: CRC Press; 2009.
32. Ciprofloxacin hydrochloride. National Center for Biotechnology Information. PubChem Database. <https://pubchem.ncbi.nlm.nih.gov/compound/Ciprofloxacin-hydrochloride> . Accessed November 14, 2019.
33. British Pharmacopoeia Commission. Ciprofloxacin hydrochloridum. <https://www.mendeley.com/catalogue/ciprofloxacin-hydrochloridum-cisapride-monohydrate-cisapridum-monohydricum/>. Published 2005. Accessed November 20, 2017.
34. Niazi SK. *Handbook of Pharmaceutical Manufacturing Formulations: Compressed Solid Products*. New York, NY: CRC Press LLC; 2009.
35. Kogawa AC, Salgado HRN. Quantification of doxycycline hyclate in tablets by HPLC-UV method. *J Chromatogr Sci*. 2013;51:919-925.